Research Project co-funded by the
European Commission
Research Directorate-General
6th Framework Programme
FP6-2005-Global-4
Global change and ecosystems
Contract No. 036355

ECOOP IP

European COastal-shelf sea OPerational Observing and forecasting system Integrated Project

D10.1.2.1Quantify the monthly to decadal variability of climate effects on the lower trophic levels of shelf sea ecosystems

Jason Holt, Sarah Wakelin (NERC)
Momme Butenschon, Icarus Allen (PML)
Morten D. Skogen, L. R. Mathisen, (IMR)
Corinna Schrum (UBI-GFS)

ECOOP WP10

Deliverable no: D10.1.2.1

Co-ordinator:

Danish Meteorological Institute, Centre for Ocean and Ice - Denmark

Table of Content

1. PUBLISHABLE EXECUTIVE SUMMARY 4

2. INTRODUCTION 5

3. NERC-POL AND PML CONTRIBUTION 6

3.1. INTRODUCTION 6
3.2. MODEL DESCRIPTION: POLCOMS 6
3.3. MODEL DESCRIPTION: ERSEM 6
3.4. FORCING AND MODEL EXPERIMENTS 7
3.5. VALIDATION 7
3.6. INTER-ANNUAL VARIABILITY 11
3.7. RESPONSE TO CLIMATE INDICATORS 12
3.8. REFERENCES 13

4. IMR CONTRIBUTION 15

MODEL DESCRIPTION 15
4.1.1. The NORWECOM model system 15
4.1.2. Model set-up, forcing and initialization 16
4.2. MODEL VALIDATION 17
4.3. WHAT CONTROLS INTER ANNUAL VARIABILITY? 18
4.4. REFERENCES: 19

5. UIB-GFI CONTRIBUTION 22

5.1. MODEL DESCRIPTION: 22
5.2. MODEL VALIDATION: 23
5.3. QUANTIFY THE MONTHLY TO DECADAL VARIABILITY OF THE CLIMATE EFFECTS ON THE LOWER TROPHIC LEVELS OF THE SHELF SEAS-COASTAL ECOSYSTEMS 30
5.4. ASSESSMENT OF CLIMATE EFFECTS 31
5.5. BALTIC SEA 34
5.6. REFERENCES 36

6. UNIV-GDA CONTRIBUTION 38

6.1. INTRODUCTION 38
6.2. METHODOLOGY OF SIMULATIONS FOR 1970-2000 38
6.3. MODEL SET-UP 39
6.4. LONG-TERM CHANGES IN NITROGEN AND PHOSPHORUS CONCENTRATIONS 39
6.5. MODEL VALIDATION 39
6.6. CHANGES IN PRIMARY PRODUCTION IN THE BALTIC AND ITS REGIONS IN 1970-2000: RESULTS OF MODELLING 41
6.6.1. Temporal changes in primary production 41
6.6.2. Spatial distribution of primary production in the Baltic 41
6.7. CONCLUSIONS 42
6.8. REFERENCES 42

Document Change Record

Author	Modification	Issue	Date
Jason T. Holt			22/1-2010
Morten D. Skogen			31/1-2010

1. Publishable Executive Summary

This report describes three studies using multi-decadal simulations of regional coupled hydrodynamics ecosystem models. These models are used to investigate the relationship between lower trophic level marine ecosystems and biogeochemistry, and the physical environment.

The models considered here:

- POLCOMS-ERSEM Atlantic Margin Model run from 1960 to 2003 (NERC and PML)
- NORWECOM North Sea Model run from 1985-2006 (IMR)
- ECOSMO (UiB-GFI) North sea and Baltic Sea run 1980-2004 (UiB-GFI)

The POLCOMS-ERSEM model is validated using *in-situ* data from the world ocean data centre and analysed to investigate the potential long term changes in primary production across the period 1960-2004, in the context of model open boundary conditions and drift. The model experiments demonstrate a strong sensitivity of the on-shelf primary production to the oceanic nutrient boundary conditions, suggesting cross-shelf edge nutrient fluxes provide a significant source of variability. The relationship between the model results and the North Atlantic Oscillation are also considered, demonstrating a r~0.65 correlation with on-shelf nutrients and the NAO

The NORWECOM model is validated here using time series data from the Dutch coast. Correlations between model variables in a selection of ICES boxes are compared with a number of driving factors. River loads are shown to dominate coastal boxes. The relationships in open-shelf boxes are more ambiguous, although the southerly inflow is demonstrated to have an important role. The validation of the POLCOMS-ERSEM and NORWECOM models both conclude that the simulations have better skill for nutrients than chlorophyll and in open-shelf seas away from the coast.

The validation of ECOSMO presented here focuses on zooplankton and comparison with data from the continuous plankton recorder, investigating six different approaches to matching CPR records with model data. Across the North Sea the mean annual cycle shows good agreement between model and CPR. There is also good correlation with along-track variability. EOF and correlation analysis is used to relate the primary production in the North Sea to atmospheric forcing parameters. The EOF patterns tend to match the distribution of summer time stratification, while the wind speed is shows the highest correlation, particularly during the onset and breakdown of stratification. This indicates the strength of cross-thermocline mixing is an important control on primary production variability. The ECOSMO model has been further developed for use in the Baltic by inclusion of nitrogen fixing cyanobacteria.

These studies each demonstrate significant control of the inter-annual variability of shelf sea ecosystems through a range of external forcing vectors: oceanic through cross-shelf edge nutrient flux, terrestrial through variations in river nutrient loading, and atmospheric via the wind control of vertical mixing. Each of these vectors potentially mediates climatic variability and climate change.

2. Introduction

The structure and functioning of marine ecosystems are highly dependent to the physical and chemical environment in which they exist and consequently so are the goods and services that depend on these ecosystems. This has led to an increasing interest in the relationship between marine ecosystems and their environment, particularly in the context of climate variability, climate change, and direct anthropogenic impacts, from both a scientific and policy oriented perspective. The goal being to understand and eventually predict the mechanisms that mediate this relationship, i.e. how marine ecosystems respond to climatic and direct anthropogenic drivers. At a regional scale in shelf seas, the most robust tools we have for developing this understanding and formulating predictions are dynamic coupled hydrodynamic-ecosystem models. The natural starting point for these models of the ecosystem is where it is most tightly coupled to the physical and chemical environment, i.e. the planktonic trophic levels. The aim for the future might be to build representations of higher trophic levels on top of these and investigate how higher trophic levels respond to environmental change, but this is beyond the scope of the current study.

In mid- to high-latitude tidally active shelf seas, seasonal and shorter cycles tend to dominate; hence many studies of the interaction between the marine ecosystem and the physical environment have tended to focus on time scales of months to a few years. However, large scale variability and trends tend to act on longer time scales, and our ability to distinguish between natural variability on multi-annual scales (e.g. the North Atlantic Oscillation) and climate change requires multi-decadal model simulations. The response time of some important processes (e.g. shelf scale flushing and the adjustment of the benthic ecosystem) is also slow compared with the seasonal cycle and hence an analysis of these requires a multi-annual treatment.

Here we present three studies that start to investigate the relationship between lower trophic level marine ecosystems and biogeochemistry and the physical environment on decadal time scales. While providing enlightening insights to the response, these studies are far from comprehensive missing as they do a complete picture of the terrestrial, ocean and atmospheric drivers, and a representation of the response that goes beyond chemical cycling to consider ecological changes (e.g. changes to species distribution and food webs).

3. NERC-POL AND PML CONTRIBUTION

3.1. Introduction

The POLCOMS-ERSEM coupled hydrodynamic-ecosystem model has been developed over the past 10 years, a collaboration between POL, PML, high performance computer specialists at the STFC and the marine forecasting division of the UK Met Office. It is widely used in a wide range of national and European funded projects. POLCOMS-ERSEM and the model experiments are described below.

3.2. Model description: POLCOMS

POLCOMS is the three-dimensional baroclinic B-grid model described by Holt and James (2001). It is a primitive equation finite difference model, solving for velocity (u,v,w), surface elevation, ζ, potential temperature, T, salinity, S and turbulent kinetic energy, q^2 in spherical polar s-coordinates (Song and Haidvogel, 1994). The model uses forward-time-centred-space differencing, with time splitting between external (fast) and internal (slow) modes. It employs a sophisticated advection scheme (the "Piecewise Parabolic Method" , James, 1996) to minimize numerical diffusion and ensure the preservation of features even on coarse grids under oscillatory flows. This scheme also ensures positivity, is not subject to a vertical CFL restriction on the time step (James, 2000). Horizontal pressure gradients are calculated by interpolation (using a cubic-spline) onto horizontal planes to avoid the errors associated with calculating these on s-coordinates where the topography is steep. Turbulent viscosities and diffusivities are calculated using a Mellor-Yamada level 2.5 turbulence closure, but with an algebraically specified mixing length.

The Atlantic Margin application (AMM) of POLCOMS has been run operationally by the UK Met. Office since 2002, using a 1/9^o latitude by 1/6^o longitude grid (~12 km) with 42 s-coordinate levels in the vertical. In this study this application is run for 1960 as a spin-up (from initial temperature and salinity fields from the global ocean model used for boundary conditions, described below), followed by a 45-year integration for the period 1960 to 2004. The implementation of POLCOMS used here is essentially that described Wakelin et al (2009) with some modifications to the forcing described below.

3.3. Model description: ERSEM

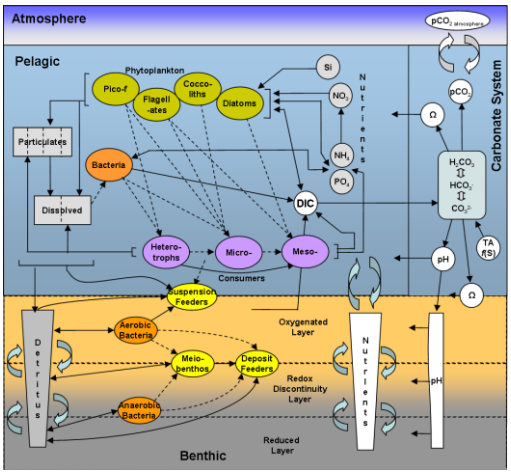

Figure 3.1 ***The benthic and pelagic components of the ERSEM ecosystem model.***

ERSEM (Figure 3.1) is a generic ecosystem model, which was originally developed and applied in the context of the North Sea. This model takes the 'functional group approach'; the biota in the ecosystem are divided into three functional types: primary producers, consumers and decomposers, which are subdivided on the basis of trophic links and/or size. Each functional group is defined by a number of explicitly modelled components: carbon, nitrogen and phosphorous and, in the case of diatoms, silicon, and the physiological and population processes are described by fluxes of these between the functional groups. Detailed descriptions of the model, and its pelagic and benthic sub-models, are given by Blackford et al. (2004), Baretta et al. (1995), Baretta-Bekker et al. (1998), Blackford (1997) and Ebenhöh et al. (1997). The parameter set used for this model simulation is that published by Blackford et al. (2004).

The calculation of non-biotic absorption differs from previous implementations of this model. Rather than using an SPM

transport model, we make use of absorption estimates from SeaWiFS. We use a mean annual cycle of monthly non-biotic absorption based on 1998-2004 SeaWiFS data on a ~9km grid; these are derived using a bio-optical model (Smyth et al., 2006). A new model variable for the inherent optical properties (*IOP*, representing CDOM and SPM concentrations) is initialised to the observed winter mean values, and advected and diffused along with the other state variables. When an observation is available, *IOP* is relaxed to this throughout the water column with a time scale of 7 days. This is a very simple interpolation based assimilation scheme that removes the myriad unknowns in trying to model SPM and CDOM directly (settling velocities, sea bed dynamics, sources/sinks, chemistry etc). Particularly it overcomes issues of model drift caused by inaccuracies in material fluxes that are apparent in multi-annual simulations. This method gives a seasonal cycle of the attenuation based on these observations, but the high frequency variability is lacking; the effects of removing this variability are the subject of future investigation.

In order to accurately model the transport of detrital material across the shelf a re-suspension flux has been included in the ERSEM model formulation. This mimics that used in the POLCOMS SPM transport model (Holt and James, 1999b). Settling only occurs when the bed stress, τ, is less than a critical value τ_{dep}, and erosion occurs when a critical stress is exceeded. So the flux of POM from pelagic to benthic models is:

$$F = w_s c(1 - \tau / \tau_{dep}) \quad \tau < \tau_{ero}$$
$$F = M(\tau / \tau_{ero} - 1) \quad \tau > \tau_{dep} \qquad (1)$$

where w_s is the settling velocity (negative), *c* the concentration of each component of POM and *M* the erosion constant.

3.4. Forcing and model experiments

Forcing is provided by the ECMWF ERA40 metrological data for surface fluxes calculated from COARE v3 bulk formulae (Fairall et al., 2003), using 6 hourly values, except for precipitation and short-wave radiation, which are daily (the latter is modulated by the diurnal cycle). Open ocean boundary conditions are taken a run of the ORCA1 application of the Nucleus for a European Model of the Ocean (NEMO) run from 1958 to 2004 (Smith and Haines, 2009), together with 15 tidal constituent from a northeast Atlantic tidal model (Flather, 1981). Elevation and depth mean current boundary conditions (tidal and 6 hourly residuals) are applied using a flux/radiation scheme. Temperature and salinity are relaxed to 5-daily NEMO data values in a four grid cell wide relaxation zone. For freshwater fluxes, daily discharge data for 322 rivers are used from the Global River Discharge Data Base (http://grdc.bafg.de/) and from data prepared by the Centre for Ecology and Hydrology as used by Young and Holt (2007). In this simulation gauged discharge data (with UK discharges corrected for ungauged flows (Marsh and Sanderson, 2003) is used where available; the gaps being filled by a mean annual cycle for each river. A mean annual cycle is used to describe the flow of low salinity water from the Baltic.

We consider two model experiments which span the period 1960 to 2004:

- S12run410. The standard model configuration using a zero-flux divergence ecosystem open boundary condition.
- S12run411. Uses nutrient boundary conditions derived from monthly mean values from the World Ocean Atlas.

Together these allow us to investigate the sensitivity of the modelled ecosystem and biogeochemistry to conditions in the wider ocean, albeit in a crude fashion.

3.5. Validation

Central to any ecosystem model study is an in-depth comparison between the simulation and contemporary observations. Given the uncertainties, and lack of consensus, in model formulation and approach this validation is crucial to provide confidence in the conclusions drawn (Allen et al., 2007). A consequence of multi-annual simulations is that a large volume of data is often available from international data centre during the simulation period for model validation. Here we use data from the World Ocean Data Centre (www.nodc.noaa.gov/OC5/WOD09/pr_wod09.html). During the simulation period there are:

- 300790 phosphate observation
- 226667 nitrate observations
- 240960 silicate observations
- 154663 chlorophyll observations

Since these data were gathered in generally unrelated observational campaigns, they do not form self-consistent time series. Hence, the approach here is to sample the daily model output at the time and location of each observation and hence form a series of independent points of comparison in a similar fashion to previous studies using data from the North Sea Project (Allen et al., 2007; Holt et al., 2005). In the present case there are sufficient data to form statistics on the model grid. Figure 3.2 shows fractional mean errors for temperature, salinity, oxygen, phosphate, chlorophyll and nitrate at each grid cell from experiment S12run410. The fractional mean error (χ) is defined by

$$\chi = \frac{2}{n} \sum \frac{A_m - A_o}{A_m + A_o}$$

The summation is over all pairs of model and observed values within a grid cell irrespective of depth or season. Figure 3.3 shows the corresponding values for experiment S12run411. There is adequate data to see general spatial patterns of model uncertainty. However since no temporal subdivision of the data is made here, these patterns are quite noisy.

All three nutrients in S12run410 show a negative bias except phosphate and nitrate in near coastal regions and in the Norwegian Trench, Kattegat and Skagerrak. Silicate shows a strong negative bias across the whole domain except around the coast of Norway and in the Kattegat and Skagerrak. The patterns of chlorophyll are very noisy, since the data is sparse and sampled from all periods of the year. There is a tendency for negative bias in some coastal regions suggesting excessive light limitation and reflecting the positive bias seen in the phosphate and nitrate. The open ocean regions south of ~50^{o}N tend to show a negative chlorophyll bias. The seas to the north and west of Scotland, the Norwegian Trench, Kattegat and Skagerrak show a positive chlorophyll bias. The other regions of the mode domain are more ambiguous.

When the climatological nutrient boundary conditions are introduced in S12run411 (Figure 3.3) there are marked changes in the biases. The bias in open-ocean silicate is substantially improved to become weakly positive. The negative bias across much of the shelf is also reduced although it still remains large in coastal regions, indicating deficiencies in the riverine silicate inputs. Phosphate across much of the domain is significantly improved as is nitrate in the open ocean, but this now shows a weak positive bias on-shelf. The negative biases in chlorophyll are generally improved, although northern regions of the model now show a systematic positive bias which is also reflected as a negative bias in oxygen.

Typical cost function values (RMS error divided by the standard deviation of the observations) on-shelf are: 7.6 for silicate, 2.3 for phosphate, 1.0 for nitrate and 1.6 for Chlorophyll. These are generally dominated by large values in the Kattegat and Skagerrak. Values in the open-ocean are somewhat improved: 1.6 for silicate, 0.8 for phosphate and nitrate, 1.0 for chlorophyll.

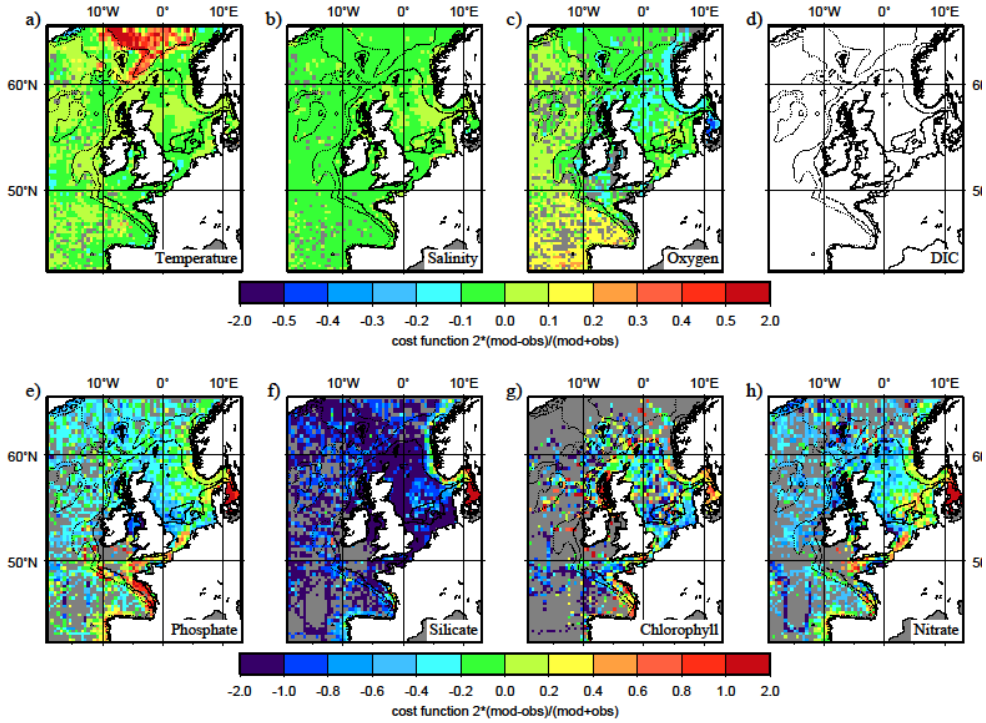

Figure 3.2 ***Fractional mean uncertainty for experiment S12run410 compared with data from WODC.***

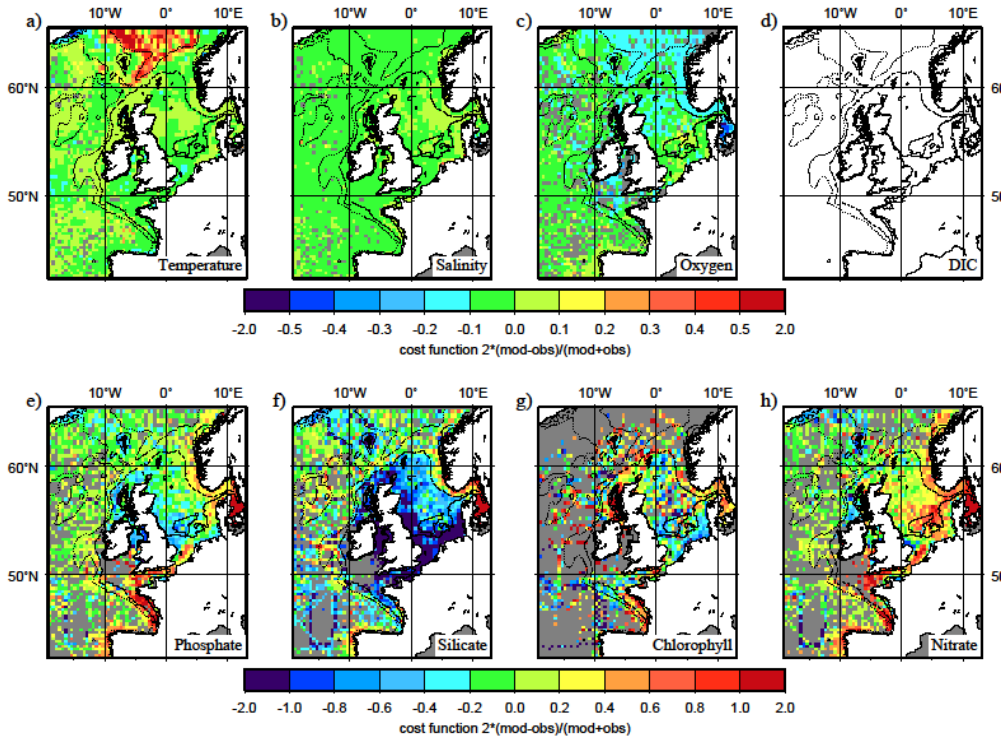

Figure 3.3 ***Fractional mean uncertainty for experiment S12run411 compared with data from WODC.***

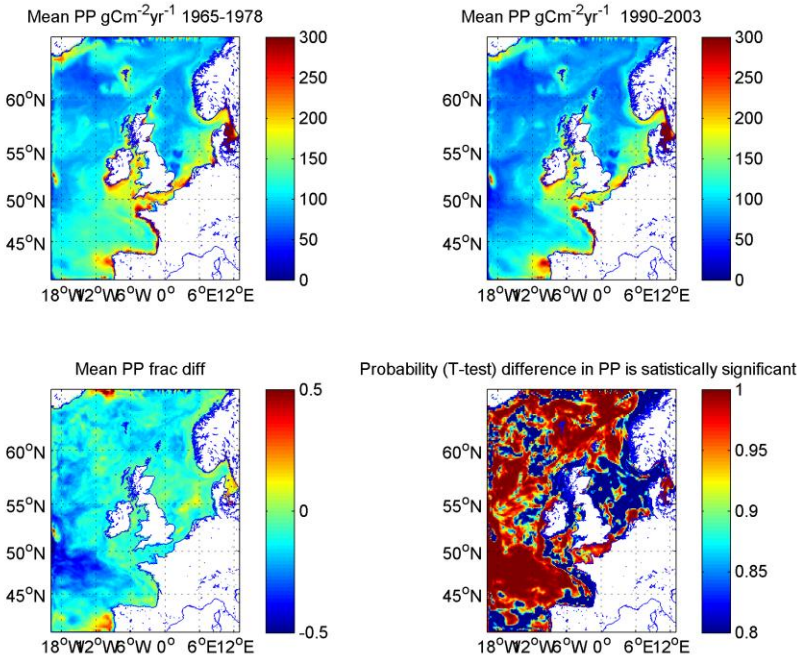

Figure 3.4 ***Mean primary production from experiment S12run410: 1990-2003 and 1965-1978, the difference between them and the statistical significance of the difference in the mean compared with the inter-annual variability.***

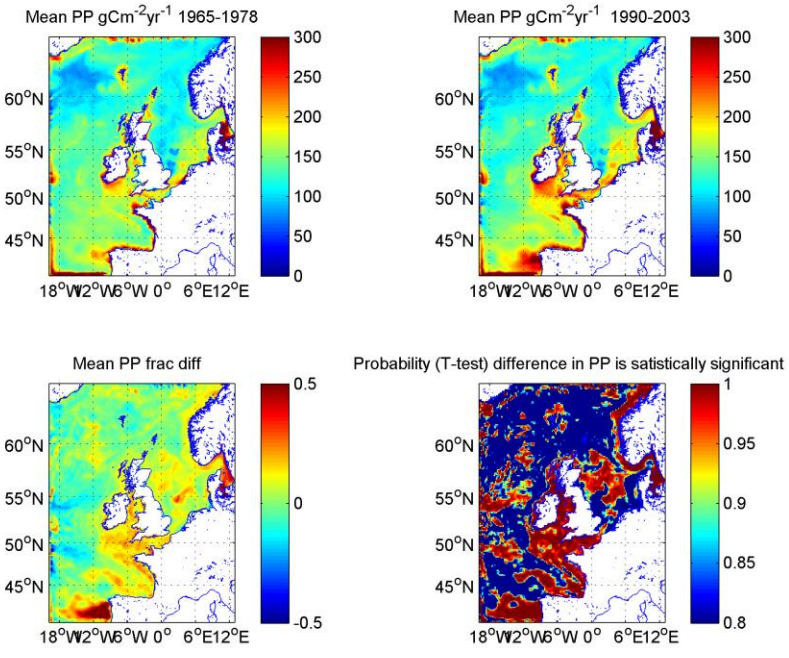

Figure 3.1 ***Mean primary production from experiment S12run411: 1990-2003 and 1965-1978, the difference between them and the statistical significance of the difference in the mean compared with the inter-annual variability.***

3.6. Inter-annual variability

A basic question regarding the marine ecosystem's response to variability in the physical and chemical environment is: have mean conditions in the present day change compared with those in the past and why? Figure 3.4 shows the mean annual primary production from S12run410 for the 14-year period 1990-2003 compared with average conditions in 1965-1978. It also shows an estimate of the statistical significance of this change using a T-test on the difference of the mean compared with a standard deviation derived from the inter-annual variability. These results show a significant decrease in the northern North Atlantic primary production and only weak changes in on-shelf primary production. Comparing this change with the inter-annual variability demonstrates that the average values in the two periods are significantly different.

However, performing the analysis on experiment S12run411 (Figure 3.5) immediately questions the robustness of this conclusion. Introducing climatological nutrient open-boundary conditions has a substantial effect on the simulation, as suggested by changes in the model biases discussed above. The deep ocean regions now show only a small, patchy increase in primary production, much of which is not statistically significant. In contrast the on-shelf primary production increases significantly, particularly in the Celtic Sea, English Channel and Irish Sea. Improvements in the nutrient fields in S12run411 described above suggest this is a more robust conclusion but is generally hampered by lack of data (e.g. in Celtic Sea), and possibly issues of model drift (see below).

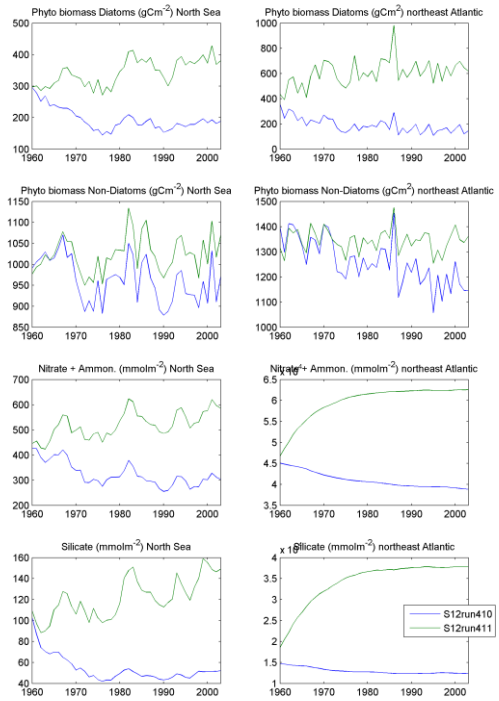

Figure 3.6 ***Time series of phytoplankton biomass (split into diatoms and non-diatoms), total inorganic nitrogen and silicate averaged over two regions: the North Sea (depths less than 200m) and the open-ocean regions north of 53.11°N.***

To further investigate the temporal evolution of these model simulations Figure 3.6 shows annual mean time series of phytoplankton biomass (split into diatoms and non-diatoms), total inorganic nitrogen and silicate averaged over two regions: the North Sea and northeast Atlantic for S12run410 and S12run411. It demonstrates a significant adjustment in the nutrient distribution in the open-ocean depending on the boundary conditions, with the run using climatologically boundary conditions tending to a higher equilibrium mean values (6.2 mmol N m^{-3} and 3.1 mmol Si m^{-3}) than the case with the zero flux-divergence boundary condition (3.8 mmol N m^{-3} and 1.2 mmol Si m^{-3}). This water column integrated property is reflected at the surface and this is apparent in the changes in the phytoplankton biomass. In S12run410 diatoms decline by ~50% over the course of the run (mostly in the first 15 years) and non-diatoms decline more steadily by ~15%. In contrast diatoms in run S12run11 increase by ~30% and non-diatoms remain constant over the course of the run. These changes in open-ocean nutrients are reflected in the nutrients and phytoplankton biomass in the North Sea. A rapid decrease in silicate in S12run410 is replaced by a steady increase in S12run411, with the diatoms following the silicate in both experiments. Non-diatoms and inorganic nitrogen show a similar but more gradual pattern with non-diatoms in S12run411 show little trend.

These experiments demonstrate the importance of the on-shelf flux of nutrients in determining shelf sea primary production on multi-decadal time-scales. Our ability to represent the processes that mediate this exchange (Huthance et al., 2009) at current model resolution needs to be assess. In addition the oceanic

regions of a shelf scale model and the open-ocean boundary conditions require careful consideration. Also apparent from these experiments are issues of model drift. It is worth noting that a drift such as that seen in the silicate here is not in itself unphysical; the particulate state is decoupled from the water volume by settling, deposition and resuspension. Hence an accumulation of concentration is possible in a constituent that enters a particulate state. This is not the case for a conservative constituent that exists purely in the dissolved state, in which case the maximum concentration is set by the initial and boundary conditions. That said this drift warrants careful future investigation in relation to the available observations and the processes that control the recycling of silicate; an immediate supposition being that a loss term is either missing from the model or inappropriately parameterized. Moreover, it is crucial to identify the time scales at which a model reaches equilibrium in order to distinguish between long-term change arising as a response to forcing and the model reaching equilibrium.

3.7. Response to Climate Indicators

The NAO is the dominant mode of winter climate variability in the North Atlantic region ranging from central North America to Europe and much into Northern Asia. The NAO is a large scale seesaw in atmospheric mass between the subtropical high and the polar low. The corresponding index varies from year to year, but also exhibits a tendency to remain in one phase for intervals lasting several years. Climatic oscillations are reflected in atmospheric modes such as the North Atlantic Oscillation (NAO). Through its influence on European weather conditions, the NAO is steering indirectly the whole European biosphere and may be seen as a proxy for regulating forces in aquatic and terrestrial ecosystems; such relationships between long-term biological/planktonic time-series and the NAO have also been found (e.g. Fromentin and Planque, 1996; Reid et al., 1998). George et al. (2004) analysed the direct and indirect effects of NAO weather conditions on four lakes in Britain from data which was recorded between 1961 and 1997. Especially the changes of lake conditions in the two smaller lakes, Esthwaite Water and Blelham Tarn, could directly be correlated to NAO Index variation; with Nitrate ($r = -0.6$) and chlorophyll ($r = -0.5$) being inversely correlated to the NAO. Through the comparison of meteorological measurements and NAO Index, they found that in years with positive NAO Index, winter weather conditions in Britain were extremely mild and wet and that biological activity was increased during these years, which caused a higher nitrate assimilation in the surrounding catchment of the lakes, and therefore reducing the input of nitrate. Similar analysis of our simulations indicates that model winter nitrate ($r = -0.3$) and chlorophyll ($r = -0.2$) is also inversely correlated with the NAO.

Principle component analysis of the average winter nutrient concentrations for nitrate, phosphate and silicate produces two main components representing 66% (PC1) and 33(%) of the variability (Figure 3.7), While PC1 has no relationship with the NAO, PC2 shows a significant correlation. ($r = 0.65$), suggesting PC2 is may be representative of the impact of direct atmospheric forcing. Firstly this indicates the NAO is present in the atmospheric forcing and that the hydrodynamic model is integrating the signal and passing it to the ecosystem model. Secondly it indicates that the model may be able capture some observed relationships between the NAO and nutrients.

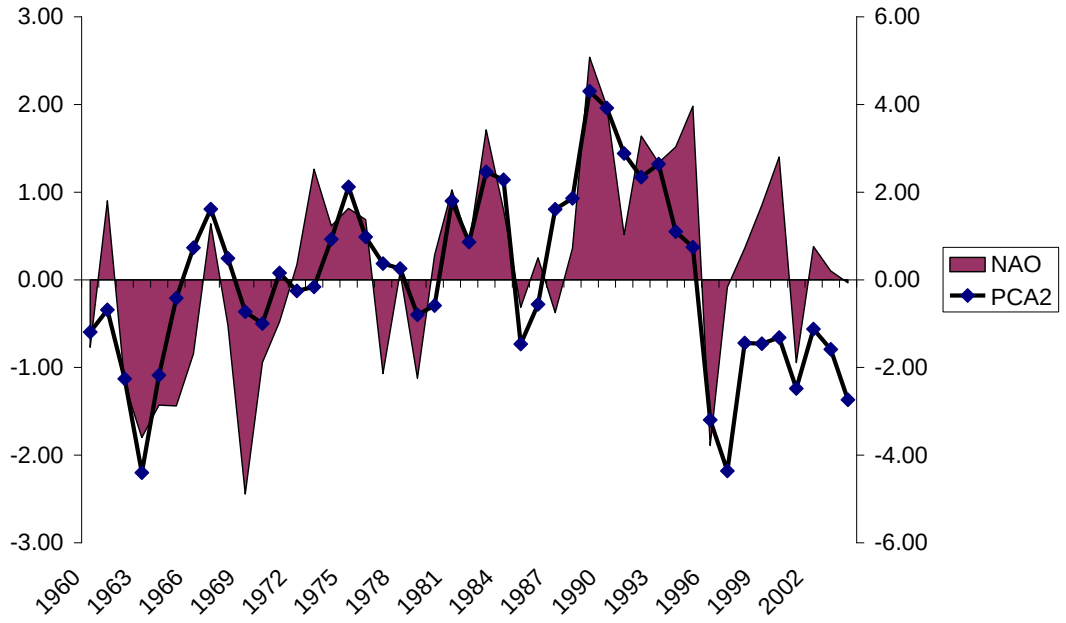

Figure 3.7. Relationship between PC2 of the model (depth <200m) winter nutrients (S12run410) and the NAO.

3.8. References

Allen, J.I., Holt, J.T., Blackford, J.C. and Proctor, R., 2007. Error quantification of a high-resolution coupled hydrodynamic-ecosystem coastal-ocean model: Part 2. Chlorophyll-a, nutrients and SPM. Journal of Marine Systems, 68(3-4): 381-404.

Baretta-Bekker, J.G., Baretta, J.W., Hansen, A.S. and Riemann, B., 1998. An improved model of carbon and nutrient dynamics in the microbial food web in marine enclosures. Aquatic Microbial Ecology, 14(1): 91-108.

Baretta, J.W., Ebenhoh, W. and Ruardij, P., 1995. The European Regional Seas Ecosystem Model, a complex marine ecosystem model. Netherlands Journal of Sea Research, 33: 233-246.

Blackford, J.C., 1997. An analysis of benthic biological dynamics in a North Sea ecosystem model. Journal of Sea Research, 38(3-4): 213-230.

Blackford, J.C., Allen, J.I. and Gilbert, F.J., 2004. Ecosystem dynamics at six contrasting sites: a generic model study. Journal of Marine Systems, 52: 191-215.

Ebenhoh, W., Baretta-Bekker, J.G. and Baretta, J.W., 1997. The primary production module in the marine ecosystem model ERSEM II, with emphasis on the light forcing. Journal of Sea Research, 38(3-4): 173-193.

Fairall, C.W., Bradley, E.F., Hare, J.E., Grachev, A.A. and Edson, J.B., 2003. Bulk parameterization of air-sea fluxes: updates and verification for the COARE algorithm. Journal of Climate, 16: 571-591.

Flather, R.A., 1981. Results from a model of the northeast Atlantic relating to the Norwegian Coastal Current. In: R.S.a.M. Mork (Editor), The Norwegian Coastal Current Vol. 2, pp. 427-458.

Fromentin, J.M. and Planque, B., 1996. Calanus and environment in the eastern North Atlantic. 2. Influence of the North Atlantic Oscillation on C-finmarchicus and C-helgolandicus. . Mar. Ecol. Prog. Ser. , 136: 111-118.

Holt, J.T., Allen, J.I., Proctor, R. and Gilbert, F., 2005. Error quantification of a high resolution coupled hydrodynamic-ecosystem coastal-ocean model: part 1 model overview and assessment of the hydrodynamics Journal of Marine Systems, 57: 167-188.

Holt, J.T. and James, I.D., 1999b. A simulation of the Southern North Sea in comparison with measurements from the North Sea Project. Part 2: Suspended Particulate Matter. Continental Shelf Research, 19: 1617-1642.

Holt, J.T. and James, I.D., 2001. An s-coordinate density evolving model of the North West European Continental Shelf. Part 1 Model description and density structure. Journal of Geophysical Research, 106(C7): 14015-14034.
Huthance, J.M., Holt, J.T. and Wakelin, S.L., 2009. Deep ocean exchange with the west-European shelf seas Ocean Sciences, 5: 1-13.
James, D., 2000. A high-performance explicit vertical advection scheme for ocean models: how PPM can beat the CFL condition. Applied Mathematical Modelling, 24(1): 1-9.
James, I.D., 1996. Advection schemes for shelf sea models. Journal of Marine Systems, 8: 237-254.
Marsh, T. and Sanderson, F., 2003. Derivation of daily outflows fromHydrometric Areas. National River Flow Archive. . Unpublished manuscript.
Reid, P.C., Planque, B. and Edwards, M., 1998. Is observed variability in the long term results of the Continuous Plankton Recorder survey a response to climate change. Fish. Oceanogr. , 7: 282-288.
Smith, G. and Haines, K., 2009. Evaluation of the S(T) assimilation method with the Argo dataset. . Quarterly Journal of the Royal Meteorological Society, 135: 739-756.
Smyth, T.J., Moore, G.F., Hirata, T. and Aiken, J., 2006. A semi-analytical model for the derivation of ocean color inherent optical properties: description, implementation and performance assessment. Applied Optics, 45: 8116-8131.
Song, Y. and Haidvogel, D., 1994. A semi-implicit ocean circulation model using a generalized topography-following coordinate system. Journal of Computational Physics, 115: 228-244.
Wakelin, S.L., Holt, J.T. and Proctor, R., 2009. The influence of initial conditions and open boundary conditions on shelf circulation in a 3D ocean-shelf model of the North East Atlantic. Ocean Dynamics, 59: Doi: 10.1007/s10236-008-0164-3.
Young, E.F. and Holt, J.T., 2007. Prediction and analysis of long-term variability of temperature and salinity in the Irish Sea. Journal of Geophysical Research, 112: doi:10.1029/2005JC003386, 2007.

4. IMR CONTRIBUTION

The IMR contribution is published in: Skogen, M.D. and Mathisen, L.R. (2009). Long term effects of reduced nutrient inputs to the North Sea. *Estuarine, Coastal and Shelf Science* **82** (2009) 433–442. Below is a summary of the main results for D10.1.2.1

Model Description

4.1.1. The NORWECOM model system

The NORWegian ECOlogical Model system (NORWECOM) is a coupled physical, chemical, biological model system (Aksnes et al., 1995; Skogen et al., 1995; Skogen and Søiland, 1998) applied to study primary production, nutrient budgets and dispersion of particles such as fish larvae and pollution. The model has been validated by comparison with field data in the North Sea/Skagerrak in e.g. Svendsen et al. (1996), Skogen et al. (1997), Søiland and Skogen (2000), Skogen et al. (2004), Hjøllo et al. (2009).

The physical model is based on the three-dimensional, primitive equation, time dependent, wind and density driven Princeton Ocean Model (POM). The model is fully described in Blumberg and Mellor (1987). In the present study the model is used with a horizontal resolution of 10 km (Fig. 4.1). In the vertical, 20 bottom following sigma layers are used. The chemical–biological model is coupled to the physical model through the subsurface light, the hydrography and the horizontal and the vertical movement of the water masses. The prognostic variables are dissolved inorganic nitrogen (DIN), phosphorus (DIP) and silicate (SI), two different types of phytoplankton (diatoms and flagellates), two detritus (dead organic matter) pools (N and P), diatom skeletals (biogenic silica) and oxygen. The processes included are primary production, respiration, algae death, remineralization of inorganic nutrients from dead organic matter, self shading, turbidity, sedimentation, resuspension, sedimental burial and denitrification. Phytoplankton mortality is given as a constant fraction, and is assumed to account also for zoo-plankton grazing which in this context is included as a forcing function. The material produced by mortality is partly regenerated through the detritus pool, but a fraction of 10% is instantly regenerated as dissolved inorganic nitrogen (in nature as ammonium) and 25% as phosphorus available for uptake by phytoplankton (Garber, 1984; Bode et al., 2004).

Particulate matter has a sinking speed relative to the water and may accumulate on the bottom if the bottom stress is below a certain threshold value and likewise resuspension takes place if the bottom stress is above a limit. Remineralization takes place both in the water column and in the sediments. The bottom stress is due to both currents (including tides) and surface waves. To calculate the wave component of the bottom stress, data from DNMI's operational wave model, WINCH (SWAMP-Group, 1985; Reistad et al., 1988), are used. Parameterization of the biochemical processes is taken from literature based on experiments in laboratories and mesocosms, or deduced from field measurements (Pohlmann and Puls, 1994; Aksnes et al., 1995; Gehlen et al., 1995; Lohse et al., 1995, 1996; Mayer, 1995).

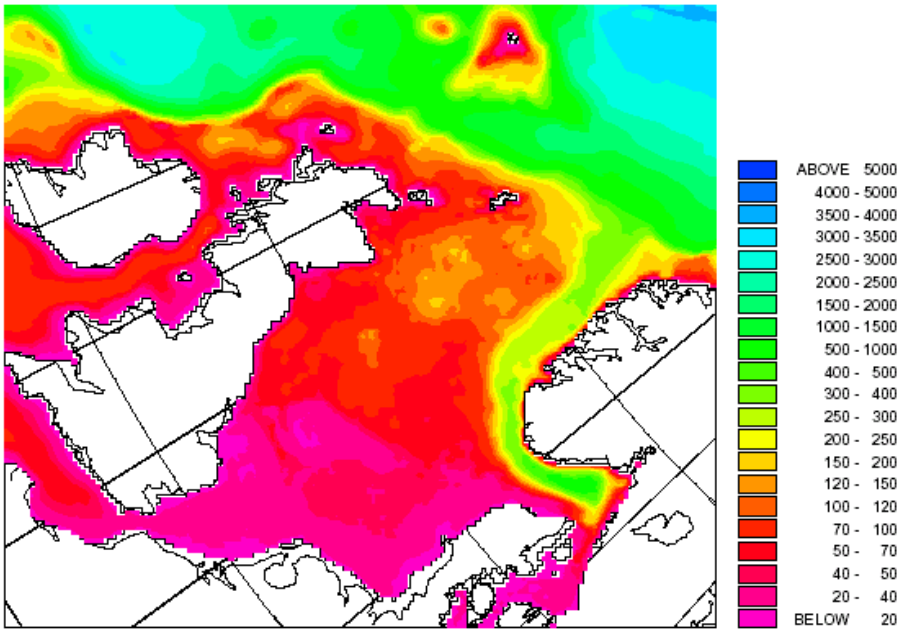

Figure 4.1. *Model area and bathymetry, with colors indicating depth in meters.*

4.1.2. Model set-up, forcing and initialization

Two simulations will be presented here. One reference with fixed 1985 river data, and one realistic using real rivers. The realistic simulation has been run for a 22 year period (1985–2006), and the one with fixed river data for 11 years (1985-1995), both starting on 1 January 1985. After a four year spin-up (running 1985 four times) to ensure that the model is in equilibrium with the boundary conditions and river loads, the years 1985 through 2006 (1995) were run sequentially.

The forcing variables are six-hourly hindcast atmospheric pressure fields and wind stress from the European Center for Medium-Range Weather Forecasts (ECMWF), four tidal constituents at the lateral boundaries and freshwater run-off. Surface heat fluxes (short and long wave radiation, sensible and latent heat fluxes), are calculated using data available from the ECMWF archive. Initial values for velocities, water elevation, temperature and salinity are taken from monthly climatologies (Martinsen et al., 1992). Interpolation between these monthly fields are also used at the open boundaries, except at the inflow from the Baltic where the volume fluxes have been calculated (Stigebrandt, 1980) from the modelled water elevation in Kattegat and the climatological monthly mean freshwater run-off to the Baltic. To absorb inconsistencies between the forced boundary conditions and the model results, a 7 gridcell ‘‘Flow Relaxation Scheme’’ (FRS) zone (Martinsen and Engedahl, 1987) is used around the open boundaries in all simulations.

Irradiation and light in the water column is modelled using a formulation based on Skartveit and Olseth (1986, 1987), using surface solar radiation data from ECMWF as input data. Nutrients (inorganic nitrogen, phosphorus and silicate) are added to the system from the rivers and from the atmosphere (only inorganic nitrogen). Monthly mean river data (freshwater and nutrient loads) are processed from data that originates from Rijkswaterstaat (Belgium and the Netherlands), Arbeitsgemeinschaft fu r die Reinhaltung der Elbe and Niedersa¨chsisches Landesamt fur Okologie (Germany), National Environmental Research Institute (Denmark), The Swedish Meteorological and Hydrological Institute and Swedish University of Agriculture (Sweden), the Norwegian Water Resources and Energy Directorate and the Norwegian State Pollution Control Authority (Norway), while data from the U.K. are processed from raw data provided by the Environment Agency (S. Painting, CEFAS, pers. comm). Retention factors for inorganic nitrogen (10%) and phosphorus (50%) are taken from Anon. (1992). In addition some extra freshwater is added along the Norwegian and Swedish coast to fulfill requirements to estimated total freshwater run-off from these coastlines (Egenberg, 1993). The model assumes saturated oxygen

conditions at the surface boundary. The initial nutrient fields are derived and extrapolated/interpolated (Ottersen, 1991) from data (obtained from ICES) together with some small initial amounts of algae. Nutrient data (monthly means) measured in the Baltic (ICES) are used for the water flowing into Kattegat.

4.2. Model validation

The mean surface nitrate and phosphate winter concentrations and mean growing season chlorophyll-a at two stations outside the Dutch coast (Noordwijk 10 (N10, 10 km off the coast) assumed to represent coastal water and Noordwijk 70 (N70, at 70 km), assumed to be central North Seawater) were taken from Waterbase (http://www.waterbase.nl), and have been compared to similar values from the model simulation (Fig. 4.2).

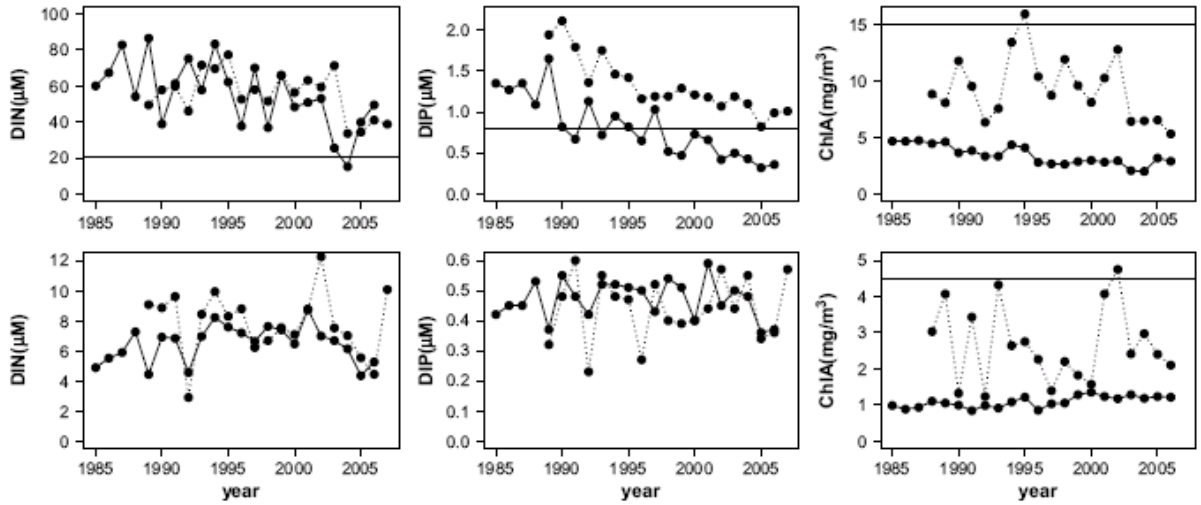

Fig. 4.2. *Comparison of winter nutrients and mean growing season chlorophyll at Noordwijk station 10 (coastal water, upper) and 70 (central North Sea water, lower). Model (solid line) and measurements (dotted line). Straight lines are the OSPAR elevated assessment levels (OSPAR 2005).*

For the winter nutrients there is a good agreement (approximately 10%) between the modelled and measured long-term means for three out of four cases. Only for DIP at N10, the measurements are almost a factor 2 higher than the model. This indicates that the retention in the estuaries for phosphate used in the model (50%) is too high at least for the nearby Rhine, Meuse and North Sea Canal that are measured very near their North Sea entry points. Chlorophyll data show a large discrepancy and less variability in the model compared to the measurements. For N10 both model and data show a decline. An interesting observation is that there is no correlation between mean growing season chlorophyll-a at N10 and N70, neither in the model nor in the data. It should be noted that while the model outputs are monthly means, the number of data points varies from 1 to 5 per month between the years, and there are large day to day variations. As an example, the very high DIN value at N70 in 2002 (from2 observations), is dominated by the value on February 14 that year (14.4 µM).

Examining the full time series (all observations) of DIN, DIP and chlorophyll-a from N10 and N70 shows a high frequency variability with a strong seasonal signal. Therefore, to make a proper comparison of the full data set, the monthly mean deviation from the monthly averages of both model and data (using the model output from those dates when observations are available), has been compared. There is a good agreement ($p < 0.01$) between model and observations for DIP at N10 and DIN and chlorophyll-a at N70. There is also an agreement ($p < 0.05$) for DIP at N70. For DIN and chlorophyll-a at N10 no significant relationship can be established. From this it can be concluded that the model does better for nutrients than chlorophyll, and that the model performance is better off the coast then at the coast.

4.3. What controls inter annual variability?

An analysis of the model outputs have been done on results from five different boxes in the southern North Sea, two offshore and three coastal. The boxes (three Dutch and two German) noted NLC2, NLC3, NLO2, GC1 and GO2 have previously been delineated and used by the 2nd workshop of OSPAR ICG-EMO held in Lowestoft, September 2007. Their positions are shown in Fig. 4.3.

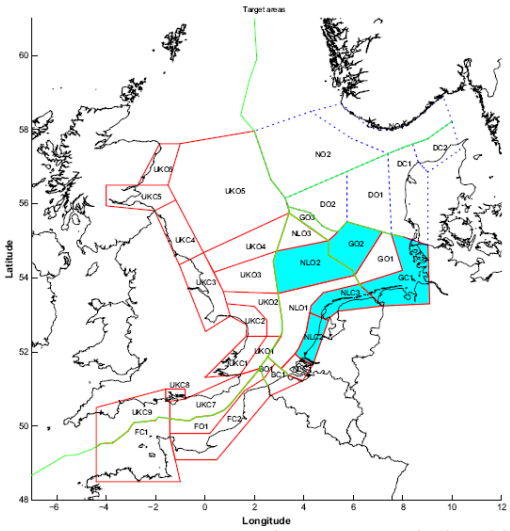

Fig. 4.3. *Target areas: GC1, GO2, NLC2, NLC3 and NLO2, as defined by OSPAR ICG-EMO (OSPAR, 2008).*

Examining the different simulations, makes it possible to partly distinguish the importance of different forcing to the assessment variables (Table 1). The overview shows that the coastal boxes are to a large extent controlled by the river loads. The exception is oxygen minimum in GC1 where the only significant relationship found was to the local winds. For the open ocean boxes the relationships are less clear. The oxygen result for the German Bight is partly in agreement with Hickel (1998) who concluded that potential eutrophication effects from the Elbe river loads may be completely overridden by hydrographic effects. Oxygen deficiency in the outer German Bight since 1980 on the other hand, has been linked with eutrophication (von Westernhagen et al., 1986) in agreement with the present model findings. The southern inflow has the second largest impact (by number) and contributes to various degrees to all assessment variables, in agreement with Breton et al. (2006) and Lacroix et al. (2007) who report on the relationship between the inflow through the English Channel and phytoplankton in the Belgian Coastal Zone. The North Atlantic Oscillation (NAO) that has an impact on both large scale winds and inflows, is only found to influence the oxygen levels. The low dependency of NAO compared to the high control by the river loads is in agreement with Radach and Pätsch (2007), who found no correlations between NAO and the river discharges. The low dependency of the northern inflow (partly controlled by the NAO, see e.g. Winther and Johannessen (2006)) compared to the southern inflow, is in agreement with the work by Kauker and von Storch (2000) who found that the North Sea surface circulation could be represented by two circulation modes. The first is a gyre flushing the entire North Sea, and the latter a bipolar pattern with short lived southern and northern gyres with opposite directions. This indicates that the variability of the assessment parameters is more strongly correlated to local events than large scale patterns like the NAO. The most interesting observation is the very few significant relationships between winter nutrients, chlorophyll and oxygen in the boxes. This means that it is hard to give predictions of one assessment variable locally from measurements of another one. This result is in agreement with McQuatters-Gollop et al. (2007) who concluded that despite decreasing nutrient concentrations, chlorophyll-a continues to increase, suggesting that climatic variability and water transparency may be more important than nutrient concentrations to phytoplankton production. That there are no relationships to winter DIN while some were found for DIP, implies that phosphorus tends to be the limiting nutrient at the present spatial and temporal scale in agreement with other studies (Skjoldal, 1993; Aure et al., 1998).

Forcing factor	EcoQO assessment indicator				
	Winter DIN	Winter DIP	Winter N:P	Chl_{mean}	Oxy_{min}
NAO	0	0	0	0	all but GC1
Inflow N	0	0	0	NLO2	0
Inflow S	NLC2	NLC2, NLO2	GC1, GO2, NLC3	GC1, NLC2	all but GC1
Local winds	–	–	–	–	all boxes
Winter DIN	–	–	–	0	0
Winter DIP	–	–	–	GC1, NLC3	NLC3
Winter N:P	–	–	–	GC1	GO2, NLC2
Chl mean	–	–	–	–	0
River loads	GC1, NLC2, NLC3	GC1, NLC2, NLC3	GC1, NLC2, NLC3	all but NLO1	all but GC1

Table 1 *Significant relationships (p<0.05) between forcing factors and assessment parameters for the boxes. River loads are of either N or P. Local winds are August winds in the southern North Sea. Inflow N(orth) is modelled transport through a section from Orkney to Utsira (Norway) for various periods, and inflow S(outh) is modelled net flow through the English Channel. The river loads and winter nutrient forcing relationships are taken from the realistic simulation, while the other ones are from the reference run. 0 indicates no relationships, – is not tested.*

4.4. References:

Aksnes, D., Ulvestad, K., Balino, B., Berntsen, J., Egge, J., Svendsen, E., 1995. Ecological modeling in coastal waters: Towards predictive physical-chemical-biological simulation models. Ophelia 41, 5–36.

Aure, J., Danielssen, D., Svendsen, E., 1998. The origin of Skagerrak coastal water off Arendal in relation to variations in nutrient concentrations. ICES Journal of Marine Science 55, 610–619.

Blumberg, A.F., and Mellor, G.L., 1987. A description of a three-dimensional coastal ocean circulation model. In: Heaps, N. (ed), Three-Dimensional Coastal Ocean Models, Vol.4. American Geophysical Union, DC, USA, 1-16.

Breton, E., Rousseau, V., Parent, J., Ozer, J., Lancelot, C., 2006. Hydroclimatic modulation of diatom/phaeocystis blooms in nutrient-enriched Belgian coastal waters (North Sea). Limnology and Oceanography 51 (3), 1401–1409.

Egenberg, B., 1993. The relationship between hydrographical variability in coastal water and meteorological and hydrological parameters. M.Phil. thesis, Geophysical Institute, University of Bergen, Norway, 73pp, in Norwegian.

Hickel, W., 1998. Temporal variability of mirco- and nanoplankton in the German Bight in relation to hydrographic structure and nutrient changes. ICES Journal of Marine Science 55, 600–609.

Hjøllo, S., Skogen, M., Svendsen, E., 2009. Exploring currents and heat within the North Sea using a numerical model. Journal of Marine Systems 78, 180–192, doi: 10.1016/j.jmarsys.2009.06.001.

Kauker, F., von Storch, H., 2000. Statistics of synoptic circulation weather in the North Sea as derived from an multiannual OGCM simulation. Journal of Physical Oceanography 30, 3039–3049.

Lacroix, G., Ruddick, K., Gypens, N., Lancelot, C., 2007. Modelling the relative impact of rivers (Scheldt/Rhine/Seine) and Western Channel waters on the nutrient and diatoms/phaeocystis distribution in Belgian waters (Southern North Sea). Continental Shelf Research 27, 1422–1446.

Martinsen,E,A., Engedahl,H.,1987. Implementing and testing of a lateral boundary scheme as a open boundary conditions in a barotropic ocean model. Coastal Eng (11) 603-627.

Martinsen, E. A., Engedahl, H., Ottersen, G., Ådlandsvik, B., Loeng, H., Balino, B., 1992. MetOcean MOdeling Project, Climatological and hydrographical data for hindcast of ocean currents. Tech. rep. 100, The Norwegian Meteorological Institute, Oslo, Norway, 93pp.

McQuatters-Gollop, A., Raitsos, D., Edwards, M., Pradhan, Y., Mee, L., Lavender, S., Attrill, M., 2007. A long-term chlorophyll data set reveals regime shift in North Sea phytoplankton biomass unconnected to nutrient trends. Limnology and Oceanography 52 (2), 635–648.

OSPAR, 2005. Ecological quality objectives for the greater North Sea with regard to nutrients and eutrophication effects. OSPAR Eutrophication series: 229/2005, 33 pp.

OSPAR, 2008. Revised draft assessment of the predicted environmental consequences for problem areas following nutrient reductions. Report on the 2nd OSPAR ICG-EMO workshop, OSPAR EUC08/5/2-E(L), 51 pp.

Radach, G., Pätsch, J., 2007. Variability of continental riverine freshwater and nutrient inputs into the North Sea for the years 1977–2000 and its consequences for the assessment of eutrophication. Estuaries and Coasts 30 (1), 66–81.

Skartveit, A., Olseth, J.A., 1986. Modelling slope irradiance at high latitudes. Solar Energy 36 (4), 333–344.

Skartveit, A., Olseth, J.A., 1987. A model for the diffuse fraction of hourly global radiation. Solar Energy 37, 271–274.

Skjoldal, H., 1993. Eutrophication and algal growth in the North Sea. In: Della Croce, N.F. (Ed.), Symposium Mediterranean Seas 2000. Universita di Genova, pp. 445–478.

Skogen, M., Moll, A., 2005. Importance of ocean circulation in ecological modeling: An example from the North Sea. Journal of Marine Systems 57 (3-4), 289-300.

Skogen, M.D., Søiland, H., 1998. A User's guide to NORWECOM v2.0. The NORWegian ECOlogical Model system. Tech. rep. Fisken og Havet 18/98. Institute of Marine Research, Pb.1870, N-5024 Bergen,Norway 42pp.

Skogen, M.D., Svendsen, E., Berntsen, J., Aksnes, D., Ulvestad, K.B., 1995. Modelling the primary production in the North Sea using a coupled 3 dimensional Physical Chemical Biological Ocean model. Estuarine, Coastal and Shelf Science, 41, 545-565.

Skogen, M.D., Svendsen, E., Ostrowski, M., 1997. Quantifying Volume Transports during SKAGEX with the Norwegian Ecological Model system. Cont. Shelf Res. 17(15), 1817-1837.

Skogen, M.D., Søiland, H., Svendsen, E., 2004. Effects of changing nutrient loads to the North Sea. J. Mar. Syst. 46(1-4), 23-38.

Stigebrandt, A.,1980. Barotropic and baroclinic response of a semi-enclosed basin to barotropic forcing of the sea. In:Freeland, H.J., Farmer, D.M., Levings, C.D. (eds), Proceeding of the NATO Conference on Fjord Oceanography. PlenumPress, New York, 141-164.

Svendsen, E., Berntsen, J., Skogen, M.D., Ådlandsvik, B., and Martinsen, E., 1996. Model simulation of the Skagerrak circulation and hydrography during SKAGEX. J. Mar. Syst. 8(3-4), 219-236.

Søiland, H., Skogen, M.D., 2000. Validation of a 3-D biophysical model using nutrient observations in the North Sea. ICES J.Mar.Sci.57(4), 816-823.

von Westernhagen, H., Hickel, W., Bauerfeind, E., Niermann, U., Kroncke, I., 1986. Sources and effects of oxygen deficiencies in the south-eastern North Sea. Ophelia 26, 457–473.

Winther, N., Johannessen, J., 2006. North Sea circulation: Atlantic inflow and its destination. Journal of Geophysical Research 111, C12018. doi:10.1029/2005JC003310.

5. UIB-GFI CONTRIBUTION

5.1. Model Description:

The model employed is the coupled 3-D model ECOSMO (ECOSystem Model, Schrum et al., 2006a, 2006b). The model ECOSMO includes a non-linear primitive equation hydrodynamical module based on a model HAMSOM (Schrum and Backhaus, 1999) and a module calculating biogeochemistry (Schrum et al., 2006a). The coupled model is applied to a system of the North Sea and the Baltic Sea with a horizontal resolution of ~10km, 20 z-levels with 5m resolution in upper 40m layer, and a time step of 20min. The hydrodynamic module includes estimations of local air-sea turbulent exchanges and a sea-ice model (Schrum and Backhaus, 1999). The turbulent vertical exchange is calculated by an algebraic first order k-ε model (Schrum, 1997a). The model has a free surface and a variable bottom layer thickness. The standard prognostic variables of the hydrodynamic block are temperature, salinity, relative sea surface elevation, the 3-D transport field, vertical exchange coefficients, turbulent air-sea exchange, ice compactness, the level of ice thickness and ridging ice thickness, and ice transport velocities.

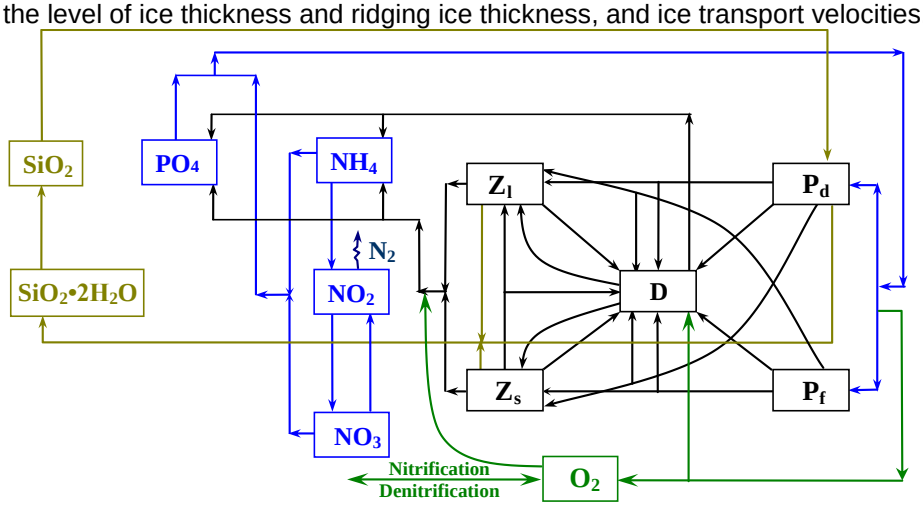

Figure 5.1. A scheme of the simulated ecosystem in ECOSMO. Modeled state variables include phytoplankton: diatoms (P_d) and flagellates (P_f); zooplankton: herbivores (Z_s) and omnivores (Z_l); detritus (D); ammonium (NH_4); Nitrite (NO_2); Nitrate (NO_3); phosphate (PO_4); silicate (SiO_2); biogenic opal ($SiO_2 \bullet 2H_2O$);
oxygen (O_2).

The biological module interactively coupled with the hydrodynamic core describes interactions between 12 state biological and chemical variables (Fig.5.1). The calculation of a modeled productive cycle is based on a simulation of three principle macro nutrient cycles, which are the nitrogen, phosphorus and silicon cycles. Phyto- and zooplankton are also included, each consists of 2 functional groups. Organic matter is resolved by functional groups of diatoms, flagellates, herbivorous and omnivorous zooplankton and detritus. The model concept is based on bulk formulations; transfer of organic matter between trophic levels and interactions between other state variables are calculated in carbon units using the constant Redfield ratio.

The model is forced by NCEP 6-hourly meteorological data, monthly river runoff, daily means of sea surface elevations with tidal dynamics (M_2, S_2 and O_1) resolved at each model time step, and climatic monthly means of temperature and salinity (Janssen et al., 1999) prescribed at the open boundaries.

Initial conditions for hydrodynamics were climatologic temperature and salinity in January (Janssen et al., 1999) after a model spin up of one year.

Modelled biogeochemistry is simulated based on initial conditions set at the beginning of model integration (1st of January), which are climatic conditions for the nutrients and slightly decreased winter seasonal plankton values available from WOA01 (Conkright et. al, 2002). Open boundaries are provided with climatic monthly means for nutrients (WOA01). Open boundary conditions for phyto- and zooplankton, detritus and biogenic opal are not available with necessary spatial-temporal resolution from public sources and, therefore, they were reconstructed based on corresponding local modelled values influenced by inflow of nutrients and then directly by local transport. The major difficulties encountered when performing a multi-year simulation are related to uncertainties in the total biogeochemical budget, which includes organic matter and nutrients. To avoid biases in the long-term dynamics of biogeochemistry, which may increase during long-term model integration due to accumulative effects of the uncertainties, we preformed this model run as series of annual cycles. The integration of the biogeochemical block started from 1st of January each year with the fixed initial conditions (taken from WOA01) without a spin-up phase.

5.2. Model Validation:

Earlier model validations have been performed for this set-up for physics, nutrients and phytoplankton. Hence our aim during the first year of ECOOP was to perform a validation of zooplankton dynamics on the seasonal but as well on the interannual time scale, which has not yet been performed. The data source used for validation was the CPR data set, which has been extensively described in the literature (e.g. Batten et al., 2003, Richardson et al., 2006). Here, plankton is filtered through a square aperture of 1.61 cm² onto a constantly moving band of silk with a mesh size of 270 µm. Samples represent 10 nautical miles of tow and approximately 3m^3 of filtered water. Alternate samples are analysed in the laboratory for plankton abundance and taxonomy. Cell counts are performed in numerical categories, resulting in semi-quantitative estimates of abundance.

For zooplankton counts, it was therefore not feasible to sum up all identified taxa but rather make a selection of one functional group. Because of their outstanding ecological importance and their relatively good catchability we obtained the abundance values for various copepod species from stage CV-CVI. For this group we assume that a consistent fraction of their in-situ abundance is sampled and that their numbers reflect the overall spatial and temporal patterns in the zooplankton community. Copepodite abundances were additionally transformed into biomass values by using a standard length-weight relationship for copepods/ zooplankton (Peters, 1983), which had been previously applied in the survey (see Richardson et al., 2006):

$$W = 0.08 * L^{2.1}$$

with L = total length of adult females and W = total mass in mg wet weight. The average wet weight for each species was then multiplied by its abundance (N/m³) and summed up to obtain total (copepod) biomass per m³. Finally, the wet weight was converted to Carbon weight per m³ according to Cushing et al. (1958): 1 mg plankton biomass approximately equals 0.12 mg Carbon. This conversion factor was based on 330 µm mesh samples and is consistent between different measures of zooplankton concentrations (see Postel et al., 2000).

In general, the CPR most likely underestimates absolute numbers and the degree of underestimation varies between species due to size, shape and behaviour (Clark et al., 2001; John et al., 2001; Batten et al. 2003; Hunt & Hosie, 2003; Richardson et al., 2004). Smaller plankton species with sizes less than a silk sampling mesh (270 µm) as well as those large zooplankton species because of active avoidance. Examining the retention of organisms on the silk during CPR tows found that organisms with widths <300 µm were not fully retain and that those with widths <287 µm had only 50% retention. For zooplankton,

abundances from other samplers are generally 1–40 times more than those from the CPR (Clark et al., 2001; John et al., 2001; Richardson et al., 2004).

Common difficulties in model validation against observational data appear due to different concepts and resolution of both approaches. Namely, strategies in observation as well as in lab experimental works are focused on investigations of individual species and their abundance. While, in terms of model concepts, which are bulk formulations simulating productive cycles, data expressed in units of biomass are needed. Methods developed to transfer abundances to units of biomass are not sufficiently accurate to account for non linear dependences between sizes and carbon content of single cells which vary depending on species as well as seasonally and regionally.

Furthermore, usually in model concepts biodiversity of species is parameterized within model functional groups, as it is done in ECOSMO. Since no data are available for growth rates, assimilation efficiency, food preferences etc. with respect to functional groups, model parameterisation remain generally to be purely theoretical. In order to validate a model, observational data have to be recalculated to be comparable with those functional groups formulated in a model. However, CPR data are representative for certain species. For the first time, such a partitioning has been done for CPR copepods (Richardson et al., 2006), which were separated into functional groups representing herbivores, omnivores or carnivores zooplankton.

Among the difficulties in interpretation of absolute values from CPR data set, particular difficulties were encountered when evaluating spatial-temporal variability due to the temporal and spatial scheme of CPR sampling (Fig. 5.2). The biases are caused by the general non-linearity of the data (e.g. seasonal dependence), interactions between spatial and temporal effects (e.g. seasonal patterns that vary with respect to location), and non-random sampling (e.g. only collecting night samples on a particular ferry route, change of ship routs) (Beare et al., 2003). Data are additionally biased due to collecting data not on a regular grid but on fixed ships routes, which are repeated quasi monthly but with some changes over a longer time period, e.g. occasional short breaks in tows, breaks of many years and terminations of old routes and installation of new ones (Richardson et al., 2006).

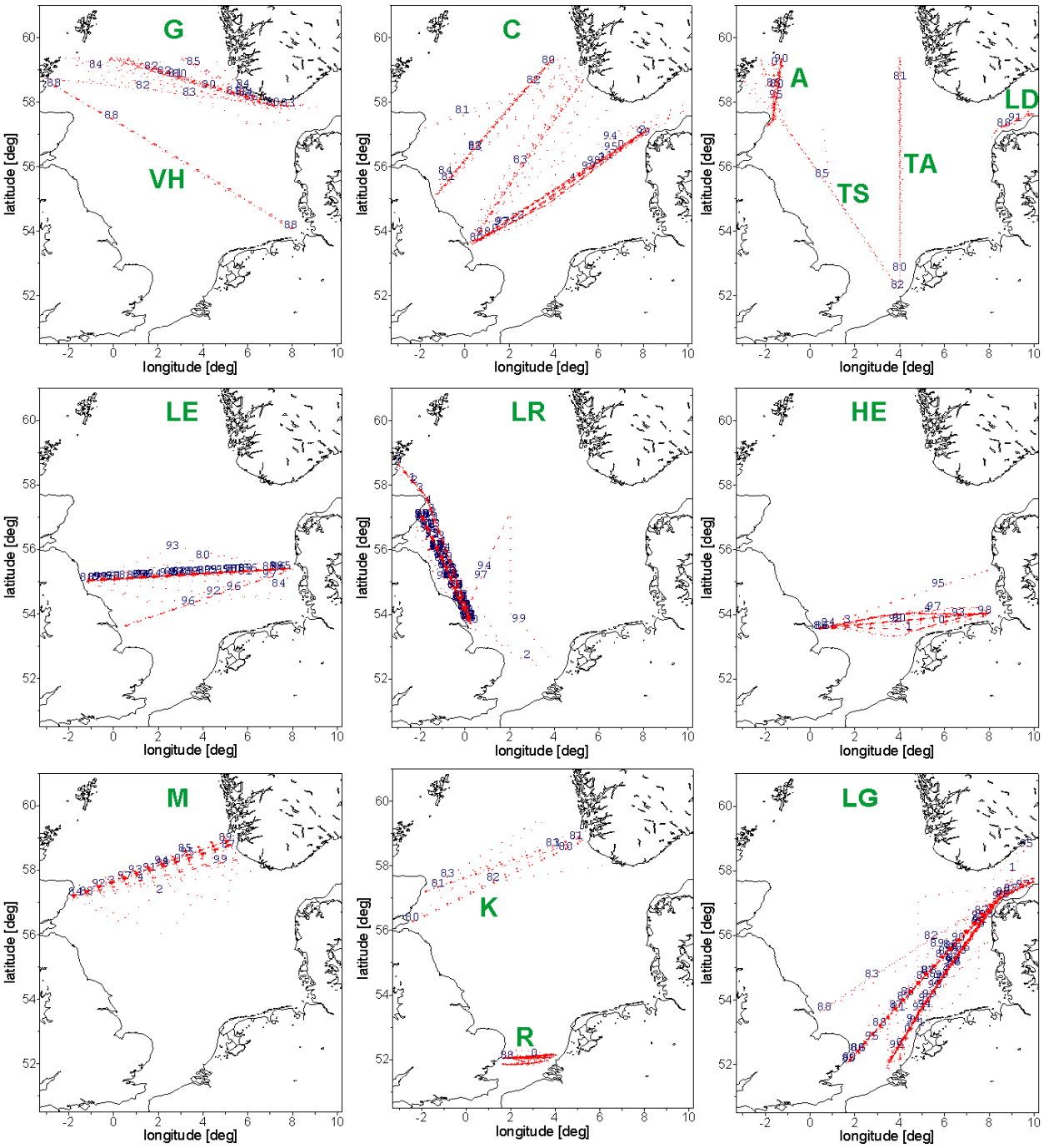

Figure 5.2. Positions of 14 CPR sampling routes performed in the North Sea over the period 1980-2004.

Therefore we based our analysis on a relevant strategy for data processing to avoid biases due to the rare CPR sampling grid. Model data were averaged in upper 10m and, then, were interpolated into locations of CPR samples taking into account dates of sampling. A linear interpolation with 5km searching radius were used, thus model values corresponding to a single CPR sample constitute a value at 1model gird cell covering area of 10km^2. Two consistent arrays of CPR data ($CPR\ \ (x, y, t)$) and model data ($MODEL\ \ (x, y, t)$) were formed to derive 1) averaged daily seasonal cycles of the pairs of chosen

parameters and 2) their long-term time-series of annual and seasonal means. For visual representation we used standardizes time-series to compare data in terms of variability.

Different concepts have been tested to synthesize the modelled and observational data and to account for the systematic deviations in concepts and lacking data on transfer coefficients. We compared model data vs observations using either (i) observed abundance vs modelled biomass, (ii) converted (standard length-weigth relation) observed biomass (carbon content) vs modelled biomass (carbon content), (iii) observed abundance vs modelled abundance proxy, for both, modelled surface values as well as vertically integrated values (Tab. 1 for details).

Table 1. Pairs of model and CPR parameters chosen for comparative analysis, and their abbreviations used in the text, Tables 2,3 and Fig. 5.3,5.4.

nn	Model	CPR	Abbreviation
1.	Omnivores biomass (***Zl***)	Copepods carbon content, (**Z**)	***Zl/Z***
2.	Total zoo biomass (***Ztot***)	Copepods carbon content, (**Z**)	***Ztot/Z***
3.	Omnivores biomass (***Zl***)	Copepods abundance, ($\mathbf{Z^A}$)	$\boldsymbol{Zl/Z^A}$
4.	Total zoo biomass (***Ztot***)	Copepods abundance, ($\mathbf{Z^A}$)	$\boldsymbol{Ztot/Z^A}$
5.	Abundance proxy ($\boldsymbol{Ztot^*}$)	Copepods abundance, ($\mathbf{Z^A}$)	$\boldsymbol{Ztot^*/Z^A}$
6.	Abundance proxy (***Ztot*****)	Copepods abundance, ($\mathbf{Z^A}$)	$\boldsymbol{Ztot^{**}/Z^A}$

To provide a consistent representation of variability of modelled total zooplankton in terms of abundance, we developed a model zooplankton abundance proxy assuming that transformation of biomass (carbon content) of smaller zooplankton results in higher abundance than that of larger zooplankton: $\boldsymbol{Ztot^A}$***= Zl+F*Zs with F=5 (Zl=omnivores, Zs=herbivores)*** was used. Based on CPR data presented and analyzed by Richardson et al. (2006), a similar conversion factor was estimated for a small selection of sampled CPR data. The factor estimated from Richardsons data was ***F=1.5***. This value has been tested here as well but gave slightly less agreement than suggesting a 5-times relation. Additionally, the proxy has been applied to vertically integrated values of modeled zooplankton ($\boldsymbol{Ztot^{**}}$***)*** to account for a possible effect of vertical zooplankton migration which is not included in the model. We note that, obviously, using of the proxy does not provide an absolute measure of abundance; however, it may describe zooplankton variability with respect to a competition between size classes.

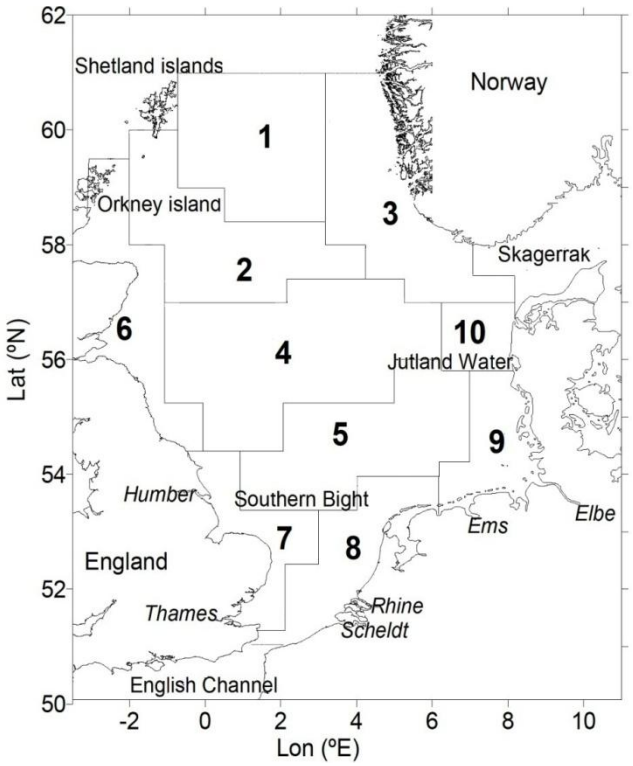

Figure 5.3. Locations of ICES- boxes.

Analyses were performed using the ICES boxes (Figure 3) and as well for the whole North Sea (Tab. 3, note box I mainly outside the model area). When performing the comparison of both, either the annual cycle as well as the inter-annual variability using the zooplankton proxy to be compared to observed abundance resulted in the highest correlations, for the respective ICES boxes as well as for the whole North Sea. Here, correlations were between 0.6 and the surprisingly high correlation of 0.91 for the whole North Sea (Fig. 5.4), with best accordance when using the vertically integrated zooplankton proxy.

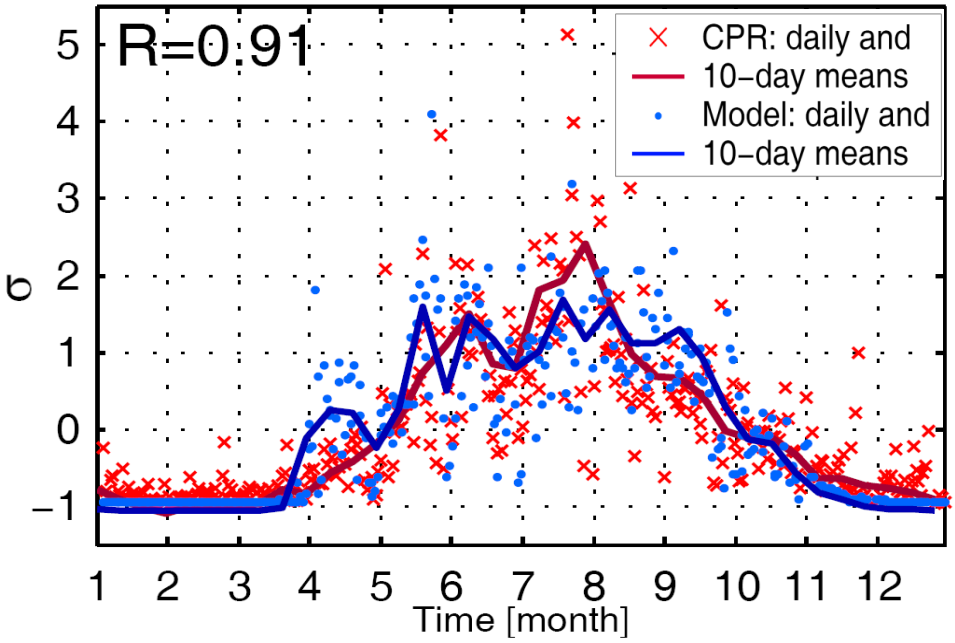

Fig. 5.4: Climatic seasonal cycle (10-day means full line, dots an crosses: daily values) of integrated zooplankton abundance proxy from model results (blue) and observed zooplankton abundance CPR data (red) in the North Sea.

Table 3. Number of data points obtained from 10-day running averaging with criterion 1 (nn1) and criterion 2 (nn2). Linear correlation coefficients derived for pairs of modeled and CPR parameters, gray fields denote low statistical significance of the correlations (p>0.01).

Area/data	*nn1*	*nn2*	*Z1/Z*	*Ztot/Z*	*Z1/Z^A*	*Ztot/Z^A*	*Ztot*/Z^A*	*Ztot**/Z*
North Sea	**37**	**37**	**0.71**	**0.71**	**0.78**	**0.84**	**0.88**	**0.91**
Box 1 (Northern NS)	5	0	0.38	-0.02	0.24	-0.01	0.00	-0.01
Box 2 (Northern NS)	**36**	**29**	**0.54**	**0.61**	**0.70**	**0.77**	**0.77**	**0.80**
Box 3 (Norwegian Tr.)	36	26	0.50	0.18	0.24	0.32	0.44	0.71
Box 4 (Central NS)	33	22	0.08	0.02	0.15	0.33	0.57	0.82
Box 5 (Central NS)	**37**	**33**	**0.50**	**0.60**	**0.67**	**0.75**	**0.81**	**0.83**
Box 6 (Scottish coast)	**36**	**31**	**0.37**	**0.37**	**0.50**	**0.59**	**0.61**	**0.75**
Box 7 (English coast)	33	23	0.60	0.61	0.54	0.71	0.74	0.74
Box 8 (Dutch coast)	**33**	**27**	**0.75**	**0.83**	**0.83**	**0.84**	**0.84**	**0.83**
Box 9 (German Bight)	27	10	0.74	0.78	0.79	0.80	0.80	0.80
Box 10 (Jutland coast)	30	17	0.31	0.37	0.40	0.46	0.50	0.60

We analyzed furthermore the long-term variability in terms of standardized time-series and standard deviations. However, in contrast to Lewis et al. (2006), we standardized the time-series of parameters at

each CPR track accounting for both their means and standard deviations derived from the overall CPR/model data domain, rather than from the time-series limited within each track:

$$A(x,y,t,Track) = \frac{data(x,y,t,Track) - mean(DATA(X,Y,T))}{\sigma(DATA(X,Y,T))}$$

where $A(x,y,t,Track)$ is resulting standardized time-series at a certain CPR track (*Track=1,..,14*) calculated from CPR or model data set, *x,y,t* are coordinates and timing of the CPR sampling grid within the track; *mean(DATA (X,Y,T))* is a mean and $\sigma(DATA(X,Y,T))$ is the standard deviation, both are derived from a data set (*DATA (X,Y,T)*, which is correspondingly CPR or model data set) with *X,Y,T* are coordinates and timing of the samples covering the whole data set. We note that this method is more informative and appropriate for evaluation of a validation based on variability at CPR tracks (and selected sub-areas), since, in addition to a comparative assessment of variability at each track, it allows for assessment of corresponding ranges of variability relative the total variances in the data sets.

The long-term times-series derived for the spring season in the total North Sea (Fig. 5.5) show relatively high correlations for both biomass (Zl/l) and abundance ($Ztot^{**}/Z^{A}$), 0.68 and 0.78, respectively. Both time-series have positive trend within the 25 year period.

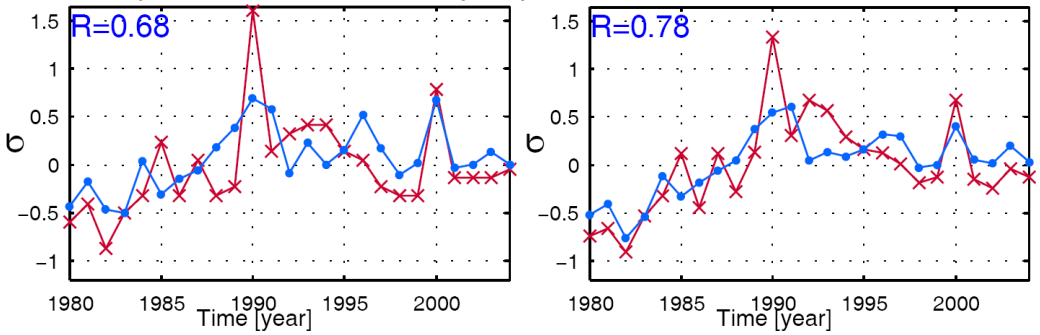

Figure 5.5. Long-term variability of zooplankton in spring (March-May) in the North Sea, 1) Zl/Z, 2) $Ztot^{**}/Z^{A}$ (see Tab. 2). Vertical axes represent variance in units of standard deviation (σ).

The corresponding time-series of annual means (Fig. 5.6) less match with correlations ~0.35 for both representations. To address spatial variability on long-term scales and its ranges at CPR tow routes, standardization relative total variability was used. It allows demonstrating that the range of variability in the entire North Sea (NS) is significantly suppressed in comparison with that ranges at the CPR route, which might be one reason for lower correlations in the entire North Sea for the annual biomass. However, the comparison of model and CPR variability demonstrates that the model is able to predict comparable ranges of variability at most CPR routes with significantly higher correlations than for the entire North Sea. Particularly, the model successfully reproduces the annual variability in the Northern and Central North Sea (routes G and C) with relatively high correlations 0.68 and 0.75, respectively. However, in the zone of Atlantic inflow (routes M and A) the long-term variability is significantly underestimated by the model due to almost climatic boundary conditions, reducing the correlation as well for the entire North Sea.

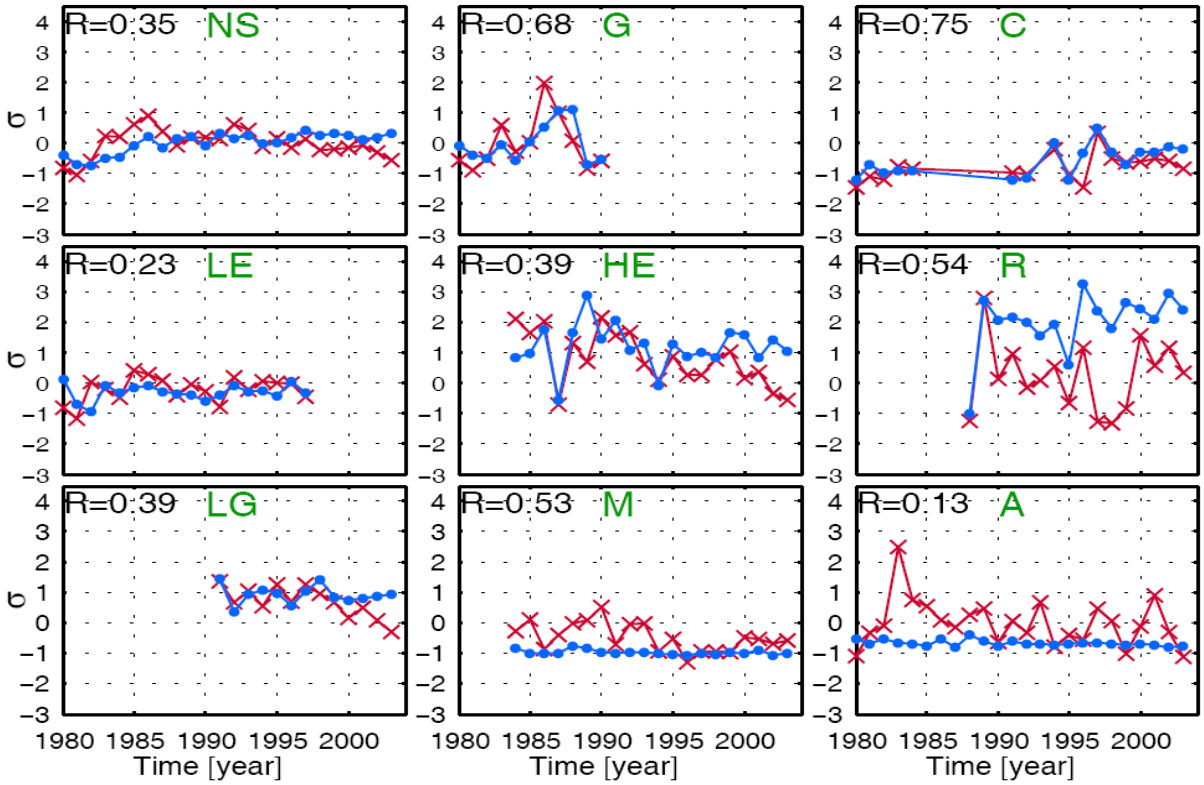

Figure 5.6. Long-term variability of annual means of zooplankton in the total North Sea and at different CPR tow routes $Ztot^{**}/Z^{A}$. Vertical axes represent variance in units of standard deviation (σ).

5.3. Quantify the monthly to decadal variability of the climate effects on the lower trophic levels of the shelf seas-coastal ecosystems

In the following we focus on investigation of the long-term variability of lower trophic level dynamics and the assessment of climate effects on the North Sea ecosystem. The investigations aimed in resolving the season-specific impact of atmospheric forcing on hydrodynamics and specifically lower trophic level dynamics. Here we used monthly mean time-series of primary production averaged in the North Sea and monthly mean 2D fields. To identify clear relationships between primary production and meteorological parameters, spatial and temporal decomposition of the data set was performed.

Monthly inter-annual variability of primary production averaged in the North Sea and in hydrodynamic important areas (the stratified Central North Sea, tidal frontal zones, the permanently mixed zone in the Southern North Sea) was cross-correlated with monthly inter-annual time-series of wind speed, air temperature, air pressure and short wave radiation. Inter-annual variability of primary production in the Central North Sea was closely and positively related with the variability of wind speed during the period of summer stratification, with strongest correlations in May (r=0.7) and August-September (r=0.8 and 0.75). Averaged production was negatively correlated with air temperature in March (r=-0.8). Using the current set-up we were unable to identify significant relationships between production and considered other atmospheric forcing parameter. Since ECOSMO underestimates strongly interannual plankton dynamics in winter due to cold starting every year (i.e. from climatic initial nutrient and biomass conditions), a fact clearly indentified by the model validation, we focus our discussion here on spring and summer conditions, a period for which ECOSMO showed good performance.

5.4. Assessment of climate effects

Here we focused on the assessment of primary production rather than discussing phytoplankton- and zooplankton biomass or secondary production, since primary production shows the most direct link to hydrodynamic variability and atmospheric forcing. We applied statistical tools to identify the linkage between modelled primary production and atmospheric forcing (NCEP reanalysis data) and thereby to evaluate climate effects on the North Sea ecosystem. We used annual and monthly mean North Sea averaged time-series of modelled primary production and wind speed, air temperature, air pressure and short wave radiation as well as 2D fields of monthly means of vertical integrated primary production resolved on the model grid. Correlation exercises employing average long-term time-series of production and those derived for atmospheric parameters, no significant relationship was found, neither for annual nor for monthly time-series.

This might be caused by complex non-linear and seasonal specific response of ecosystem dynamics and atmospheric forcing. We therefore used the decomposition of spatial and temporal signals in the 2-d primary production fields by empirical orthogonal function (EOF) analysis. The first three EOF modes describing 47% of total variability in monthly primary production were indentified (Fig. 5.7). Localized signals (Fig. 5.7, column 3) can be associated with the summer-stratified Central North Sea (27% of total variability), frontal zones (12%) and the permanently un-stratified Southern North Sea (8%). However, time-series of the principal components (Fig. 5.7, column 2) again were weakly correlated with the variability of atmospheric parameters which indicates a seasonal specific lower trophic level response to forcing.

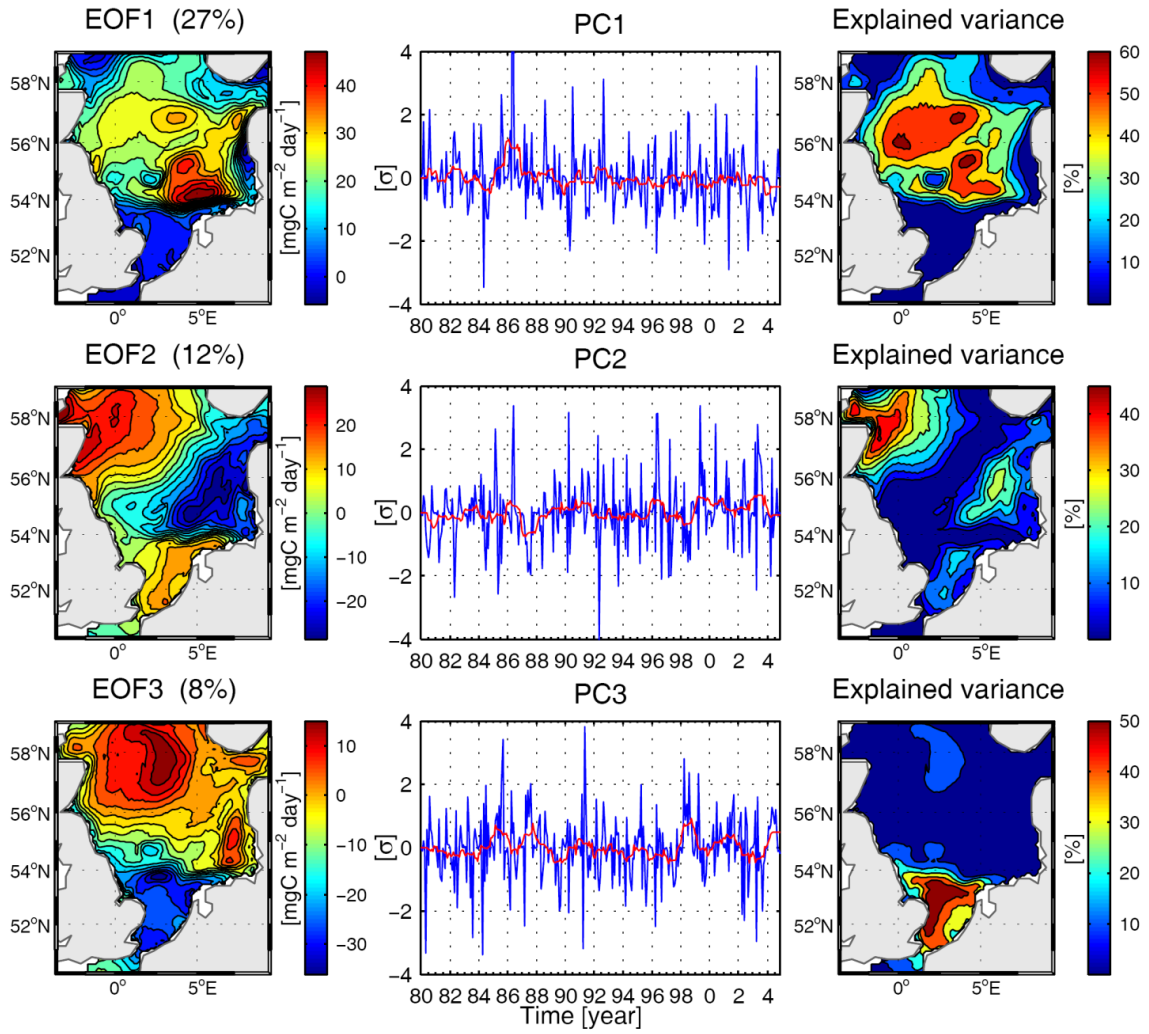

Figure 5.7. EOF analysis of anomalies of monthly vertically integrated primary with subtracted climatic seasonal cycle. First 3 EOF modes are shown from top to bottom: EOF patterns [mgC m^{-2} day^{-1}] (left), time series of principal components [units of standard deviation] (center), local explained variances [%] (right).

For temporal decomposition, inter-annual monthly time-series of primary production were separated on monthly basis. Resulting 2D arrays were similarly processed applying EOF analysis. It was found that in summer months, derived EOF patterns and locations of explained variances were close to those derived from the total variability. For instance, results from EOF analysis applied to inter-annual variability of the production distributions in May are demonstrated in Fig. 5.8. The first EOF mode contained 40% of total variability and can be related with stratification processes in the Central North Sea (Fig. 5.8, column 3). Corresponding time-series of the first principal component (Fig. 5.8, column 2) showed inter-annual variability of the pattern.

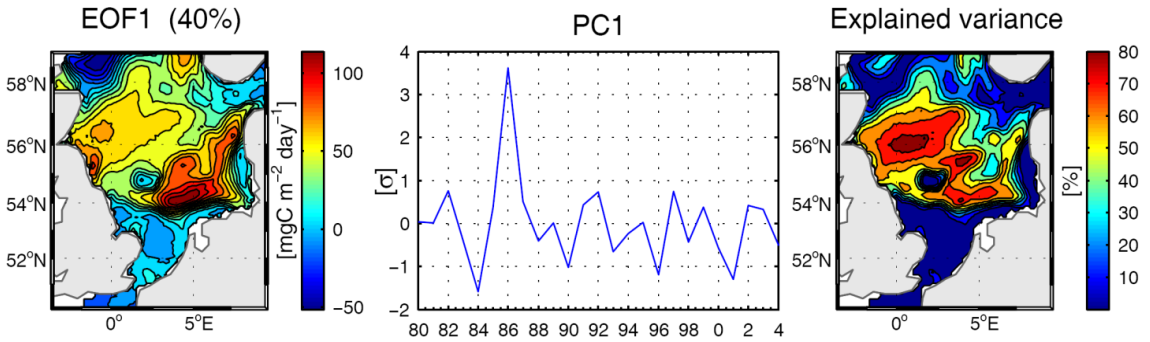

Figure 5.8. EOF analysis of anomalies of vertically integrated primary production in May. First EOF mode is shown: EOF patterns [mgC m^{-2} day^{-1}] (left), time series of principal components [units of standard deviation] (center), local explained variances [%] (right).

Searching for relationships between year to year variability of production and atmospheric parameters we used averaged in the North Sea primary production as well as derived time-series of the first three principal components. All time-series represented inter-annual variability observed in specific months and were subjected to cross-correlation analysis.

Relatively high correlations with atmospheric parameters were obtained for the averaged in the North Sea primary production and the first principal component in the respective months. Results were summarized in Fig 5.9.

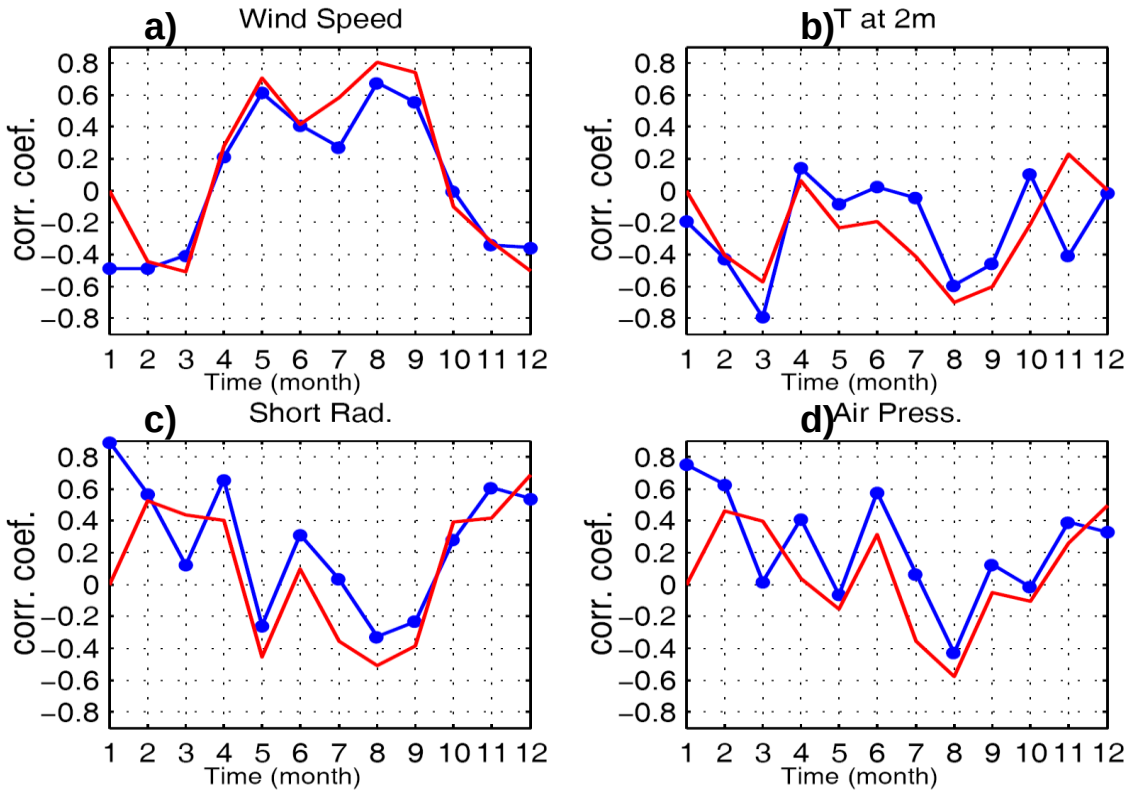

Figure 5.9. Linear correlation coefficients derived for respective months between inter-annual variability of primary production (averaged in the North Sea (blue dotted line) and first principal component (red line)) and atmospheric forcing a) wind speed, b) air temperature, c) net short wave radiation and d) air pressure.

Generally, the total North Sea averaged primary production as well as its variability derived from the first principal component showed similar correlations to atmospheric parameter, with both correlations showing a similar strong seasonal signal (Fig. 5.9). However, the strength of correlations can differ. The correlations between the first principal component which was relevant in the stratified Central North Sea and wind speed (Fig.5.9, a) derived for the period of summer stratification were the highest in comparison with other combinations and seasons. This can be related with the indirect but significant impact of wind speed on primary production via induced changes in local hydrodynamics. Increasing winds caused stronger vertical mixing and weaker stratification, thereby, controlling the vertical fluxes of new nutrients and, ultimately, resulting in enhanced primary production. This mechanism is more pronounced during the establishment of the summer stratification in May (r=0.7) and later during its breakup in August-September (r=0.8 and 0.75), while this relationship was less significant in June-July (r=0.4 and 0.6). In transition periods, spring and autumn, primary production and wind were weakly and negatively correlated.

Correlations between other considered atmospheric parameters showed lower correlation to primary production. Interestingly, in the period of summer stratification the variability of production was negatively correlated with both short wave radiation and air temperature. One possible explanation is that the direct impact of radiation on phytoplankton growth was less important than its indirect impact via influencing the stratification, i.e. increasing heating of the upper layer caused strengthening of stratification, which resulted in less productivity.

The North Sea averaged primary production was dominated by the processes in stratified areas showing a seasonal response to atmospheric forcing and generally smaller correlations. However, for the averaged production two events with remarkably high correlations were found; the high negative correlation with air temperature in March (r=-0.8) (Fig.5.9, b) and the positive correlation with short wave radiation and air pressure in January (r=~0.9) (Fig.5.9, c and d). The latter, cannot be addressed as meaningful due to ECOSMO was shown to underestimate the lower-tropic levels dynamics in the beginning of seasonal cycle.

5.5. Baltic Sea

In contrast to the North Sea, extensive summer blooms of diazotrophic cyanobacteria occur regularly in the Baltic Sea (Kahru *et al.* 2007). They are of great ecological importance, since their blooms add biological useful form of nitrogen to a eutrophicated but largely nitrogen-limited aquatic system. Therefore the NPZD-module of ECOSMO was extended by a third phytoplankton group (Fig. , representing cyanobacteria, in order to simulate ecosystem dynamics in the Baltic Sea. The parameterization of this group was based on previously developed models for the Baltic Sea published by Neumann et al. (2002) and Eilola et al. (2009).

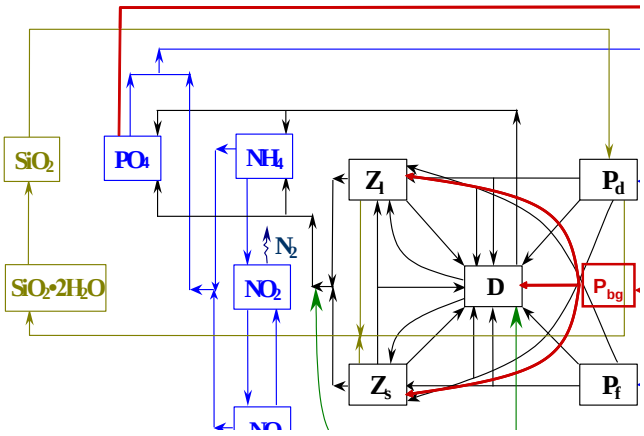

Figure 5.10. A scheme of the simulated ecosystem in ECOSMO (compare Fig. 5.1) including the additional phytoplankton group representing cyanobacteria (P_{bg}).

Due to the ability to fix nitrogen from the atmosphere growth of this group, in contrast to the other phytoplankton groups, is only limited by light and phosphorus availability. Cyanobacteria in the model are additionally featured by positive buoyancy and temperature dependent growth rates.
First results from this extended model version are shown in Figure 5.11. In contrast to the North Sea ecosystem dynamics the ratio between diatoms and flagellates in the Baltic Sea is shifted in aid of the diatom biomass as previously indicated by comparable model studies (e.g. Janssen et al. 2004, their figure 3). A pronounced peak of diatoms occurred early in the year supported by relatively high silicate concentrations. On the other hand simulated biomass of cyanobacteria is relatively low and occurs in late summer between July and August.

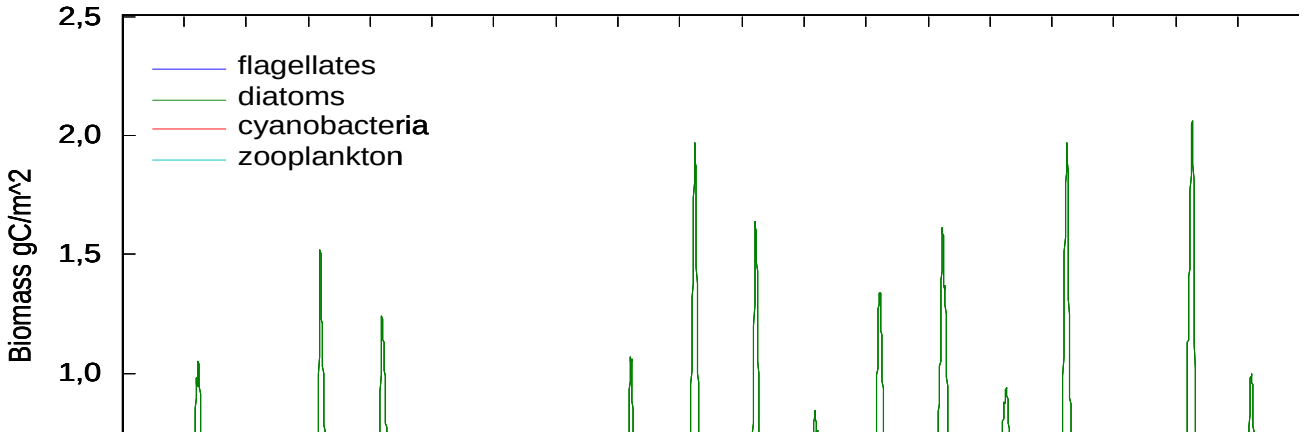

Figure 5.11. Results from a 20 year simulation with the re-parameterized ECOSMO. Baltic Sea average values g. for the 3 phytoplankton groups and the total zooplankton (small zooplankton + large zooplankton).

The annually integrated anomalies of biomass for all four groups (Fig. 5.12) indicate a slight increase in diatom biomass during the 90s, while flagellates, cyanobacteria and total zooplankton biomass show a slight opposite trend.

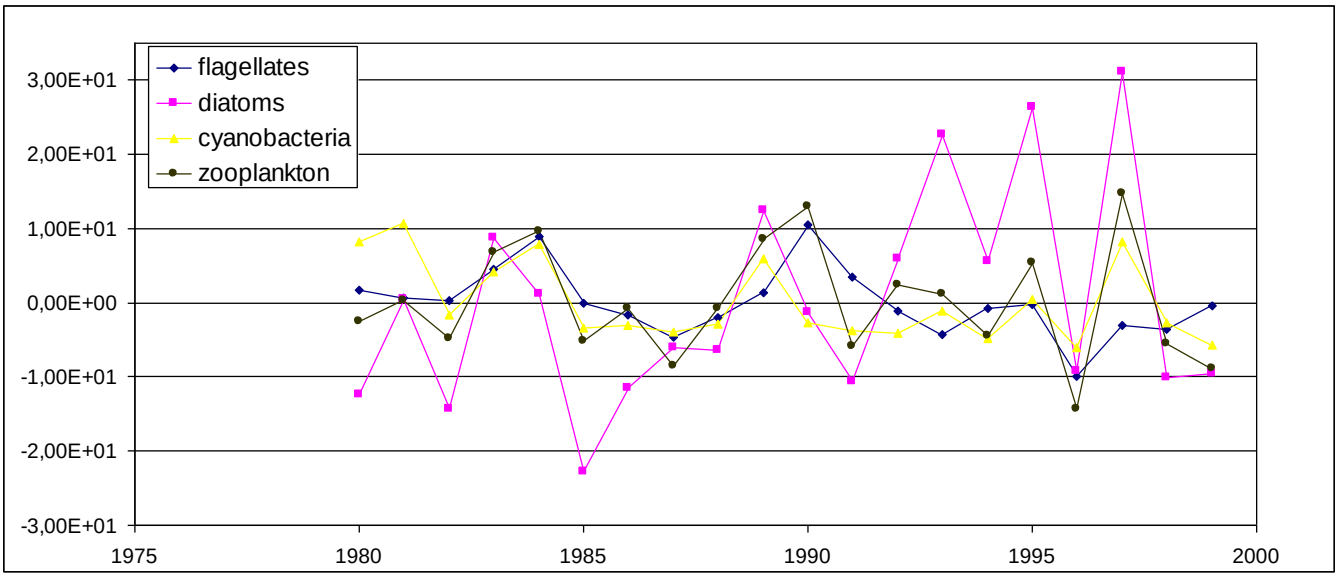

Figure 5.12. Same results as in figure 5.11 but annually integrated and displayed as anomaly to the mean value. Values are given in gC/(m^2y^{-1}).

5.6. References

Batten, S. D., Clark, R. A., Flinkman, J., Hays, G. C., John, E. H., John, A. W. G., et al. 2003. CPR sampling – the technical background, materials and methods, consistency and comparability. Progress in Oceanography, 58, 193–215.

Beare, D. J., Batten, S. D., Edwards, M., McKenzie, E., Reid, P. C., & Reid, D. G. 2003. Summarising spatial and temporal information in CPR data. Progress in Oceanography, 58, 217–233.

Clark, R. A., Frid, C. J. L., & Batten, S. 2001. A critical comparison of two long-term zooplankton time series from the central-west North Sea. Journal of Plankton Research, 23, 27–39.

Conkright, M.E., Locarnini, R.A., Garcia, .H.E., O'Brien, T.D., Boyer, T.P., Stephens, C., Antonov, J.I. 2002. World Ocean Atlas 2001: Objective Analyses, Data Statistics, and Figures, CD-ROM Documentation. National Oceanographic Data Center, Silver Spring, MD, 17 pp.

Cushing, D. H., Humphrey, G. F., Banse, K., and Laevastu, T. 1958. Report of the Committee on Terms and Equivalents. Rapports et Procèsverbaux

des Réunions du Conseil Permanent International pour l'Exploration de la Mer. 14(4):15-16. pp.

Eilola,K., Meier,H.E.M., and Almroth,E. 2009. On the dynamics of oxygen, phosphorus and cyanobacteria in the Baltic Sea; A model study. Journal of Marine Systems 75: 163-184.

Hunt, B. P. V., Hosie, G. W. 2003. The continuous plankton recorder in the Southern Ocean: a comparative analysis of zooplankton communities sampled by the CPR and vertical net hauls along 140_E. Journal of Plankton Research, 25, 1561–1579.

Janssen, F, Schrum, C, Backhaus, J, 1999. A climatological data set of temperature and salinity for the North Sea and the Baltic Sea. Dtsch. Hydrogr. Z., Suppl. 9.

Jannsen, F., Neumann, T., Schmidt, M. 2004 Inter-annual variability in cyanobacteria blooms in the Baltic Sea controlled by wintertime hydrographic conditions. Mar Ecol Prog Ser 275: 59-68.

John, A. W. G., & Reid, P. C. 2001. Continuous plankton recorders. In J. H. Steele (Ed.), Encyclopaedia of Ocean Sciences (pp. 502–512). Harcourt Press.

Kahru,M., Savchuk,O.P., and Elmgren,R. 2007. Satellite measurements of cyanobacterial bloom frequency in the Baltic Sea: interannual and spatial variability. Mar Ecol Prog Ser 343: 15-23.

Lewis, K., Allen, J. I., Richardson, A. J., and Holt, J. T. 2006. Error quantification of a high resolution coupled hydrodynamic-ecosystem coastal-ocean model: Part 3, validation with continuous plankton recorder data. Journal of Marine Systems, 63 (3-4): 209-224.

Neumann,T., Fennel,W., and Kremp,C. 2002. Experimental simulations with an ecosystem model of the Baltic Sea: A nutrient load reduction experiment. Global Biogeochem.Cycles 16.

Postel, L., Fock, H. and Hagen, W. 2000. Biomass and abundance. pp. 83 – 192. In: ICES Zooplankton Methodology Manual. Ed. by R. Harris, H.R. Skjoldal, J.Lenz, P. Wiebe and M. Huntley. Academic Press, San Diego, San Francisco, New York, Boston, London, Sydney, Tokyo: 684pp.

Richardson, A.J., Walne, A., Witt, M., Lindley, J. A., John, A. W. G. and Sims, D. W. 2006. Using Continuous Plankton Recorder Data. Progress in Oceanography, 68: 27-74.

Richardson, A. J., John, E., Irigoien, X., Harris, R. P., & Hays, G. . 2004. How well does the continuous plankton recorder (CPR) sample zooplankton? A comparison with the Longhurst Hardy plankton recorder (LHPR) in the northeast Atlantic. Deep-Sea Research I, 51, 1283–1294.

Schrum, C., 1997a: A coupled ice-ocean model for the North Sea and the Baltic Sea. Sensitivity of North Sea, Baltic Sea and Black Sea to anthropogenic and climatic changes. Nato ASI Ser., Kluwer Academic Publishers. Emin Özsoy and Alkexander Mikaelyan (Ed.), 311-325.

Peters, R. H. (1983). The ecological implications of body size. Cambridge: Cambridge University Press, 329 pp.

Schrum, C., 1997b: Thermohaline stratification and instabilities at tidal mixing fronts. Results of an eddy resolving model for the German Bight. Cont. Shelf Res., 17(6), 689-716.

Schrum, C, Alekseeva, I, St. John, M (2006a): Development of a coupled physical–biological ecosystem model ECOSMO Part I: Model description and validation for the North Sea, Journal of Marine Systems, doi:10.1016/j.jmarsys.2006.01.005.

Schrum, C, Backhaus, J O (1999): Sensitivity of atmosphere-ocean heat exchange and heat content in North Sea and Baltic Sea. A comparitive assessment. Tellus 51A. 526-549.

Schrum, C, St. John, M, Alekseeva, I (2006b): ECOSMO, a coupled ecosystem model of the North Sea and Baltic Sea: Part II. Spatial-seasonal characteristics in the North Sea as revealed by EOF analysis. Journal of Marine Systems, doi:10.1016/j.jmarsys.2006.01.004

6. UNIV-GDA CONTRIBUTION

6.1. Introduction

Task 10.1.2 was carried through at the University of Gdańsk (UoG) based on the ProDeMo, the ecosystem-oriented part of the M3D_UG model. The current, third version of the model has been markedly expanded: it contains 18 state variables and considers biogeochemical exchange processes in the water column as well as those between the water column and the atmosphere, between the water column and the sediment, and within the sediment itself. The model describes functioning of the system up to the zooplankton level in the food web. For hindcasting, it was necessary to acquire the measured N and P loads discharged into the Baltic with river run-off over 1970–2000. To validate the model results, HELCOM monitoring data held in various data banks: SMHI, SYKE (FIMR), BED, and IMWM were retrieved. To address the variability of nutrients and biological productivity in their spatio-temporal dimensions, the Baltic Sea was divided into 7 regions. The major result of the task entails modelling the long-term variability in N and P concentrations, budgets of N and P in the entire Baltic Sea and its 7 regions, and spatio-temporal variability of primary production in 1970–2000.

6.2. Methodology of simulations for 1970-2000

The third version of the ProDeMo (Kowalewski, 2007) emerged as an outcome of the ECOOP WP5 activities. To arrive at a more comprehensive description of sediment-related processes, it had been assumed that the sediment should be described by 13 layers covering the uppermost 25 cm of the sediment. In addition, the model includes pore-water processes, including diffusion transport, and the solid sediment phase which features burial and bioturbation in its surficial part. A total of 7 state variables were defined in the pore water: concentrations of inorganic nitrogen, phosphorus, and silica as well as concentrations of oxygen, hydrogen sulphide, and sulphates. In addition, to model the oxygen deficiency conditions, organic matter degradation was included.

To analyse the primary production dynamics in 1970–2000 at a regional scale, the Baltic was subdivided into 7 regions (Fig 6.1). Primary production as well as components of nutrient budget were calculated for individual regions.

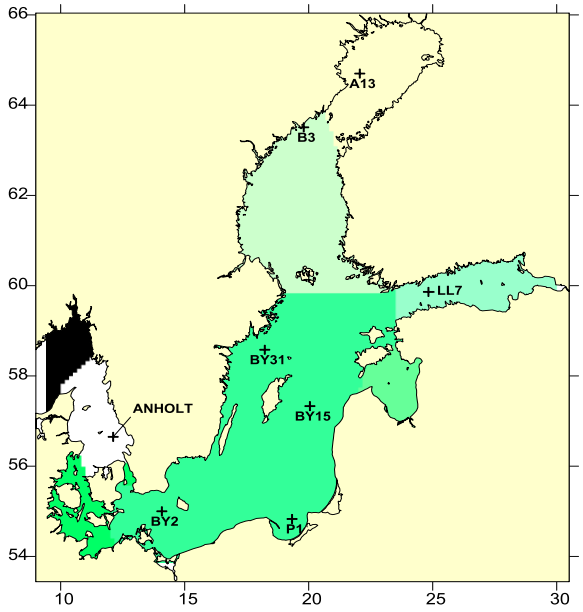

Fig. 6.1 Baltic regions and location of stations supplying data used in model validation

6.3. Model set-up

Model simulation runs were performed using meteorological data (wind speed, air temperature, atmospheric pressure, cloudiness, and humidity) from the climatic REgional MOdel (REMO) (Jacob & Podzun, 1997; Feser et al., 2001). The parameter fields, of 0.5º ×0.5º spatial resolution, were introduced at 1-h time interval. Validation of long-term simulations of the sea level, water temperature, and salinity in the Baltic, carried out using the M3D_UG hydrodynamic model (Kowalewski,1997) with the REMO data showed a close agreement with observations (Jędrasik et al., 2008).

Nutrient loads and run-offs from 168 major rivers discharging into the Baltic were included. Mean monthly run-off values over 1970-2000 were retrieved from the NEST database (http://nest.su.se/nest/). The 1970-1990 data were analysed by Stålnacke (1996), the analysis being subsequently extended to cover the 1970-2000 period (Medina et al., 2006). Dynamics of the total nitrogen (TotN) river run-off did not show any major trends (**Error! Reference source not found.**), whereas the total phosphorus (TotP) loads showed a slightly increasing trend, particularly in the Gulf of Finland.

The initial conditions for temperature, salinity, and nutrient concentrations were adopted based on averaged values recorded in winters of 1970-1997. The relevant data were retrieved from the Baltic Environmental Database (BED; http://nest.su.se/nest/). Due to the low amount of data for 1970, the initial condition was adopted based on long-term model simulations.

6.4. Long-term changes in nitrogen and phosphorus concentrations

Nitrogen and phosphorus are the most important nutrients, their concentrations in seawater being of utmost importance for the productivity of an area. The Baltic primary production is mainly nitrogen-limited, which is typical of marine areas. In some periods, e.g., during spring phytoplankton blooms, phosphates are frequently depleted. In summer, too, during intensive cyanobacterial blooms, phosphorus becomes a limiting factor, as the possible mineral nitrogen deficiency is compensated for by atmospheric molecular nitrogen (N_2) fixation. In the Gulf of Bothnia, particularly in its northern part (Bothnian Bay), a typical phosphorus limitation is observed, a situation characteristic of freshwater areas. In addition, mineral silica limitation is occasionally observed in the Gulf of Riga during diatom blooms. Silica limitation occurs, however, only locally and has no consequences for the productivity of the entire Baltic Sea.

6.5. Model validation

Analysis of long-term changes in nitrogen and phosphorus concentrations was preceded by validation of the model based on the available data for the entire Baltic.

The ProDeMo results closely approximated the observed changes in total nitrogen concentrations at station BY15 in the Gotland Deep. Until the mid-1980s, NTOT measurements showed a wide scatter, most probably related to imperfections of the measurement technique, which makes model validation difficult. Later on, the scatter of the measurement data was much less extensive, and the model produced a good fit to the data. It was only in 1994 and 1995 that the model yielded results that were slightly underestimated. In the case of inorganic nitrogen, the model predicted slightly overestimated maximum winter concentrations, but – overall – it faithfully reproduced the long-term course of changes. A still better agreement was obtained for phosphorus (Fig. 6.3), particularly for PTOT. As far as inorganic phosphorus is concerned, the observed winter concentrations were very high in some years, but the model failed to reproduce them. The simulations modelled the long-term trends of changes very well: a slight increase in NTOT concentrations in the early 1970s and a slight reduction of phosphorus concentrations in the 1990s are distinctly visible.

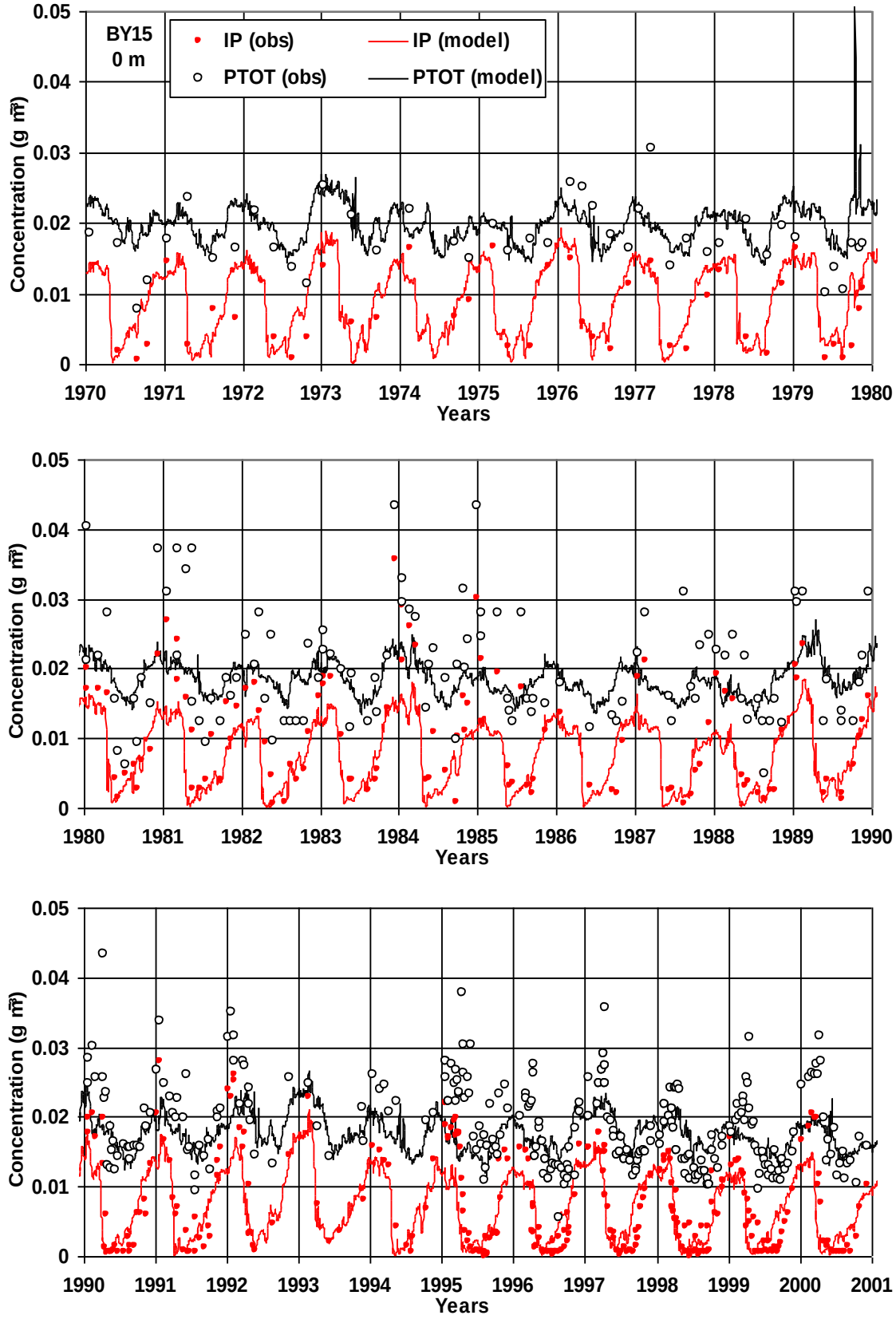

Fig. 6.2 Comparison of observed (obs) and modelled (model) concentrations of inorganic phosphorus (IP) and total phosphorus (PTOT) at BY15 in 1970–2000

6.6. Changes in primary production in the Baltic and its regions in 1970-2000: results of modelling

6.6.1. Temporal changes in primary production

The long-term simulation performed by the ProDeMo were used to estimate changes in the primary production rates in 1970–2000 both in the entire Baltic and in the individual regions.

No distinct trends were visible in the temporal dynamics of primary production (Fig. 6.4). The mean annual primary production rates in the Baltic ranged from 64 gC m^{-2} $year^{-1}$ in 1996 to 89 gC m^{-2} $year^{-1}$ in 1989. The mean annual primary production rate over 1970–2000 was c. 80 gC m^{-2} $year^{-1}$. The highest mean annual primary production rate was typical of the Baltic Proper (92 gC m^{-2} $year^{-1}$), followed by the Gulf of Riga (83 gC m^{-2} $year^{-1}$), Gulf of Finland (77 gC m^{-2} $year^{-1}$), the Danish Straits (73 gC m^{-2} $year^{-1}$), and the Kattegat (69 gC m^{-2} $year^{-1}$). The lowest rates were typical of the Gulf of Bothnia (58 and 40gC m^{-2} $year^{-1}$ in the southern and northern part, respectively). The temporal dynamics of primary production in different parts of the Baltic were distinctly correlated, which was doubtless related to the variability of the meteorological forcing in different years.

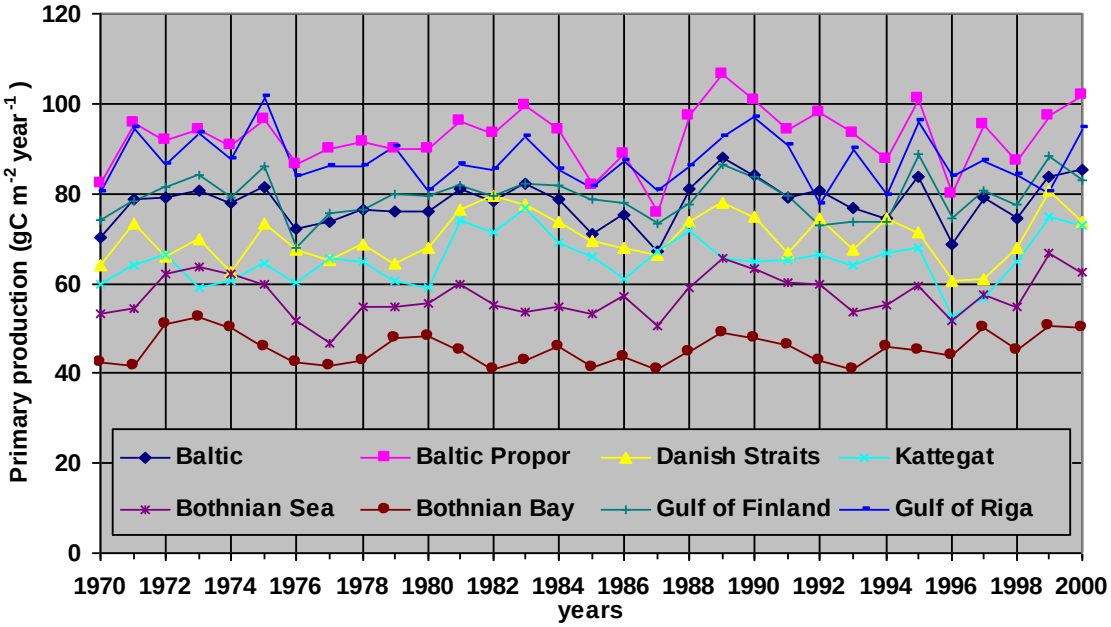

Fig. 6.4 Mean annual primary production rates in the Baltic and its regions in 1970–2000

6.6.2. Spatial distribution of primary production in the Baltic

Results of simulations performed with the ecohydrodynamic model allowed to develop a map of the mean annual primary production rate in the Baltic (Fig. 6.5). The primary production rates show a substantial spatial variability, higher rates being typical off river mouths and the open waters of the Baltic Proper. The maximum annual primary production rates of about 160 gC m^{-2} $year^{-1}$ were recorded in the southern part of the Gulf of Gdańsk, undoubtedly related to a high input of nutrients supplied by the Vistula. Elevated primary production rates can be observed locally off the mouths of the River Odra in the Pomeranian Bay and the Daugava in the Gulf of Riga. The open Baltic Proper shows bathymetric effects on the distribution of primary production rates. The effects are, however, complex, because low values occur both in shallower areas and above the Baltic deeps. In shallow areas, primary production is limited by the height of the water column supporting the production. Reduction of primary production above the deeps and enhancement in their vicinity is probably an effect of water dynamics. Such a pattern is distinctly visible both in the Bornholm and in the Gotland Deep areas.

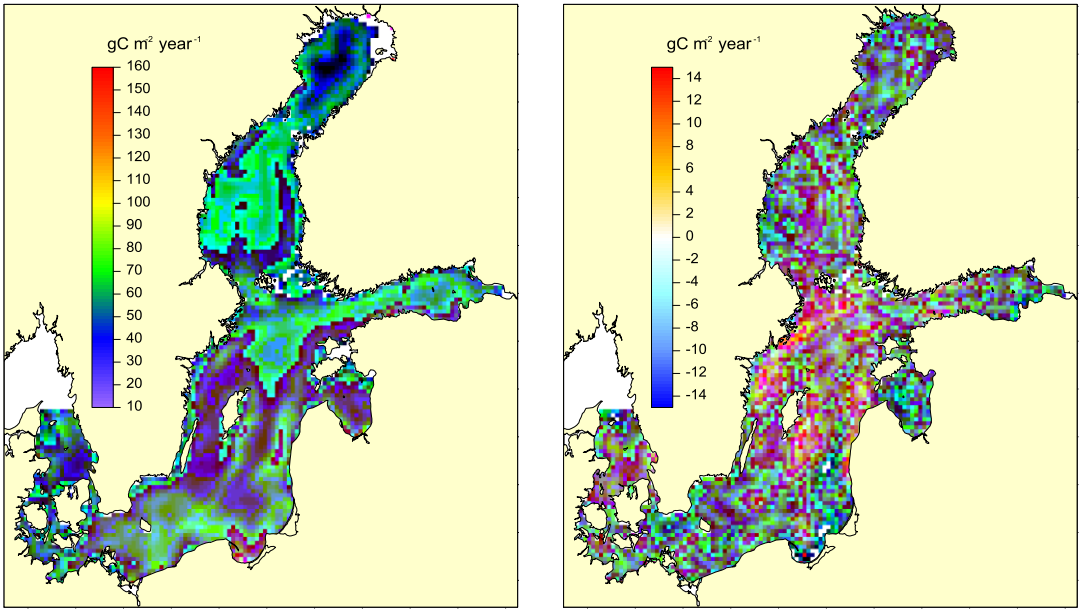

Fig. 6.5 Spatial variability of mean annual primary production rate in the Baltic in 1970-2000 (left side), a difference between mean annual primary production in the Baltic between 1990-2000 and 1970-1980 (right side)

Spatial variations in the distribution of primary production rates in 1970-2000 are also presented as a map of differences between the mean production rate in the 1990s and 1970s (**Error! Reference source not found.**). The strongest limitation of primary production is visible in the southern and eastern parts of the Baltic Proper, and also in the southern part of the Gulf of Finland. The highest increase in the primary production rate was typical of areas off the Swedish coasts in the Baltic Proper, and also off the coast of Gotland. The spatial distribution of those changes is complex, as it is most likely a net result of changes in the magnitude of nutrient supply, nutrient transport by currents, and climatic changes.

6.7. Conclusions

The long-term validation of the model showed a good agreement between the modelled and observed values of inorganic and total nitrogen and phosphorus. It was only in the Bothnian Bay and Bothnian Sea that the model showed some discrepancies relative to the observations, i.e., underestimation of nitrogen concentrations and overestimation of those of phosphorus, for which reasons the modelling results in the area should be treated with caution. On the other hand, a close agreement was observed with regard to primary production.

Analysis of the long-term simulation performed with the ecohydrodynamic model showed relatively small changes in trophic conditions prevailing in the Baltic in 1970–2000. A slight increase in nitrogen concentrations was recorded, most conspicuously in the early 1970s, and a reduction of phosphorus concentrations occurred in the last decade of the period analysed. No significant trends in the primary production were observed, changes in individual years being caused mainly by meteorological forcing. The strongest reduction of primary production in 1970–2000 was observed in the Gulf of Gdańsk, an area of the highest primary production.

6.8. References

Feser, F., Weisse, R. & von Storch, H. 2001, *Multi-decadal atmospheric modelling for Europe yields multi-purpose data*, EoS, Vol. 82, No. 28, July 10, 2001

Jacob, D. & Podzun, R. 1997. *Sensitivity studies with the regional climate model REMO*. Meteorol. Atmos. Phys., 63, 119–129

Jędrasik J., Cieślikiewicz W., Kowalewski M., Bradtke K., Jankowski A., 2008, *44 years hindcast of the sea level and circulation in the Baltic Sea*, Coastal Engineering 55, 849–860

Kannen A, Jędrasik J., Kowalewski M., Ołdakowski B., Nowacki J., 2004, *Assessing catchment-coast interactions for the Bay of Gdansk [in:] Managing the Baltic Sea*, Schernewski G., Löser N. (eds.), Coastline Reports 2, 155–165.

Kowalewski M., 2007, *Upgrade of existing model ProDeMo (ecological part of M3D_UG) – development of eco module – near bottom oxygen*, ECOOP report no: S5.2.3.7

Kowalewski M., Jędrasik J., Ołdakowski B., Nowacki J., 2003, *The impact of the Vistula river on the coastal waters of the Gulf of Gdansk, The Vistula River Catchment and the Baltic Sea Coastal Zone Case Study VISCAT*, EU Project Nº.: EVK1/2000/00510, final report

Kowalewski M.,1997, *A three-dimensional, hydrodynamic model of the Gulf of Gdańsk,* Oceanol. Stud., 26 (4), 77–98

Medina M.R., Savchuk O.P., Wulff F., 2006, *Reconstruction of riverine nutrient loads to the Baltic Sea 1970 - 2000*. Proceeding of an International Symposium "Research and Management of Eutrophication in Coastal Ecosystems", 20-23 June 2006, Nyborg, Denmark

Ołdakowski B., Kowalewski M., Jędrasik J. Szymelfenig M., 2005, *Ecohydrodynamic Model of the Baltic Sea, Part I: Description of the ProDeMo model,* Oceanologia, 47 (4), 477516

Stalnacke P., 1996, *Nutrient loads to the Baltic Sea*, Kanaltryckeriet i Motala AB, Motala, 290

Riitta Olsonen (ed), 2008, FIMR monitoring of the Baltic Sea environment. – Annual report 2007. MERI – Report Series of the Finnish Institute of Marine Research No. 62,.